

Electronic Supporting Information (ESI)

Montmorillonite clay catalyzed synthesis of functionalized pyrroles through domino four-component coupling of amines, aldehydes, 1,3-dicarbonyl compounds and nitroalkanes

Jaideep B. Bharate,^{ab} Rajni Sharma,^{bc} Subrayashstra Aravinda,^a Vivek K. Gupta,^d Baldev Singh,^{bc} Sandip B. Bharate^{ab*} and Ram A. Vishwakarma^{abc*}

^a*Medicinal Chemistry Division, Indian Institute of Integrative Medicine (CSIR), Canal Road, Jammu-180001, India*

^b*Academy of Scientific & Industrial Research (AcSIR), Anusandhan Bhawan, 2 Rafi Marg, New Delhi-110001, India*

^c*Natural Products Chemistry Division, Indian Institute of Integrative Medicine (CSIR), Canal Road, Jammu-180001, India*

^d*X-ray Crystallography Laboratory, Post-Graduate Department of Physics & Electronics, University of Jammu, Jammu-180001, India*

*E-mail: ram@iiim.ac.in; sbharate@iiim.ac.in

CONTENTS

- S1. Fe-PILC catalyst preparation and characterization
- S2. NMR data scans of all synthesized substituted pyrroles **1a-1q**
- S3. X-ray crystallography of methyl 1-(1-(4-Fluorophenyl)-2-methyl-4-phenyl-1H-pyrrol-3-yl) ethanone **1b**

S1. Fe-PILC catalyst preparation and characterization

S1a. Preparation of Fe-PILC

Ferric chloride (FeCl_3) was used in Fe-PILC synthesis. A base-hydrolyzed FeCl_3 pillaring solution was prepared using OH/Fe molar ratio of 2.0. The hydrolysis was carried out at room temperature for 16 h under continuous stirring. Montmorillonite clay K10 powder was added gradually to Fe pillared solution, providing a required mmol of Fe per gram of clay. Fe Pillared clay suspension was stirred for 3 h at room temperature to allow ion exchange between exchangeable cations of the clay and pillar precursors. The formed PILCs were centrifuged, washed, dried in air, and calcined in air at 425 °C for 3 h.

S1b. Characterization of Fe-PILC

Synthesized Fe-PILC catalyst was characterized using specific surface area determination, temperature programmed reduction (TPR), temperature programmed desorption (TPD) and scanning electron microscopy (SEM). The specific surface areas (m^2g^{-1}) of samples were estimated with the N_2 adsorption at the liquid nitrogen temperature on the Quantachrom Chem-BET 3000.

Temperature programmed reduction (TPR):

Temperature programmed reduction (TPR) profiles of catalyst precursors were collected on the Quantachrom Chem-BET 3000 apparatus equipped with a thermal conductivity detector (TCD). 50 mg samples placed in a quartz U-shaped tube were reduced in 5% H_2/N_2 flow (80 mL min^{-1}) from room temperature to 700 °C at a temperature rise of 5 °C min^{-1} . Samples were pretreated in N_2 flow (50 mL min^{-1}) at 300 °C for 2 h to remove the adsorbed water and other contaminants prior to each TPR experiment.

H_2 -Temperature-programmed reduction (TPR) profiles of the Fe – PILC catalyst are shown in Figure S1. The reduction of iron oxides takes place in three steps. In the first step, Fe_2O_3 was reduced to Fe_3O_4 and the second step involved the reduction of Fe_3O_4 to FeO which was consequently reduced to Fe. Generally FeO is not expected to appear in the TPR spectra as it has been shown that FeO is unstable compared to Fe and Fe_3O_4 . For the Fe - PILC, reduction of

Fe_2O_3 to Fe_3O_4 took place at 415 °C. The reduction of Fe_3O_4 to Fe occurred at 470 °C while the broad peak appearing between 500 to 750 was assigned to the reduction of small metal particles and mixed oxides which are difficult to reduce.

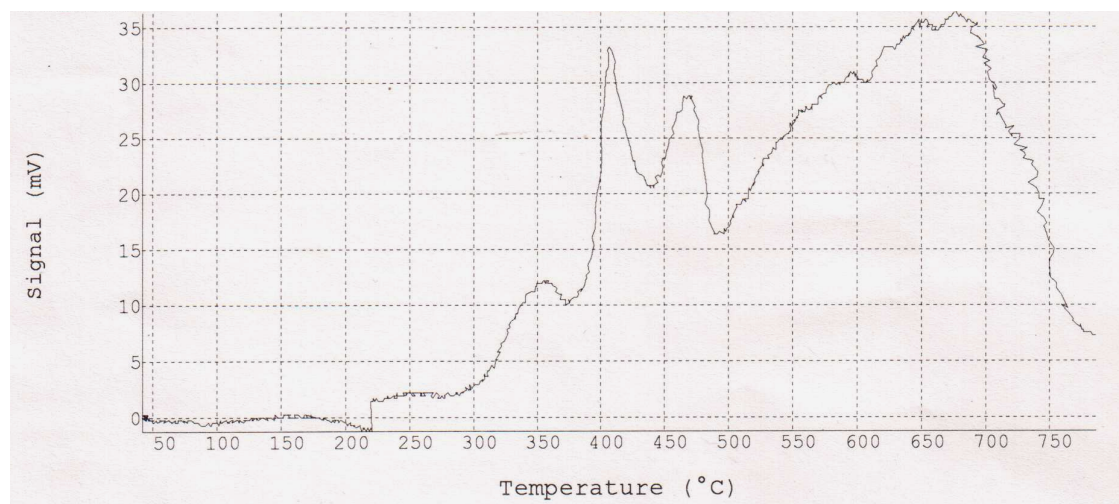


Figure S1. TPR profile of FE-PILC B catalyst

Ammonia TPD experiment:

The total acidity and acid distribution of the pillared clays was determined by ammonia TPD with the help of a CHEM BET-3000 (Quantachrome, USA) instrument in the temperature range of 30–800 °C. About 0.1 g of powdered sample was taken inside a quartz U tube and degassed at 350 °C for 1 h with ultrapure helium gas. After the sample was cooled to room temperature, NH_3 gas of 1000 ppm with N_2 gas was passed through the sample for 1 h. Then the ammonia adsorbed sample was purged with helium gas at 40 °C to remove any weakly adsorbed NH_3 on the surface. The temperature-programmed desorption of ammonia was performed between 80 and 800 °C at 10 °C /min.

Acidity was estimated as being the total amount of NH_3 released through thermal programmed desorption (TPD) per gram of dry clay sample. The number of desorbed molecules is supposed to be equal to that of the adsorption sites present on the clay surface. The acid strength is proportional to the temperature required to release the probe gas molecules. The strength distributions were expressed in terms of various amounts of ammonia desorbed under controlled temperature increase, and was estimated by TPD pattern deconvolution.

The acidity of PILC with respect to the type of pillar was observed by NH₃ TPD. The PILC contained enormously high surface acidity compared to the original clay montmorillonite. This simply indicates that the acidity of the clay is enhanced by pillaring the clay. The concentration and strength of the acidic sites of Fe – PILC catalyst have been determined by NH₃ TPD and showed in Table S1. Total acidity of the catalyst was found to be 7.91 mmol NH₃/g catalyst, which was distributed on the surface of the clay support as 47% (3.75 mmol NH₃/g catalyst), 18% (1.40 mmol NH₃/g catalyst) and 35% (2.76 mmol NH₃/g catalyst) of weak, medium and strong acidic sites.

Table S1. Distribution of activity in Fe-PILC **B** catalyst

Acidic sites	mmol NH ₃ /g catalyst	%age
Weak acidity	3.75	47.40
Medium acidity	1.40	17.70
Strong acidity	2.76	34.90
Total acidity	7.91	100

Morphology of the catalyst:

The morphology of Fe-PILC **B** catalyst was studied using JEOL.JEM100CXII electron microscope with ASID accelerating voltage of 40 KV. Figure depicts the representative SEM image of calcined Fe – PILC catalyst. The image shows that materials are randomly distributed over the support surface with flake formation. Result are supported by dispersion analysis (up to 99.4%) and average crystallite size as 11.60 Å° (CHEMBET- 3000). Fe particles are constituted by several aggregates and not by continuous film. Higher dispersed catalytic materials are able to adsorb the substrate and /or reagent to a high extent.

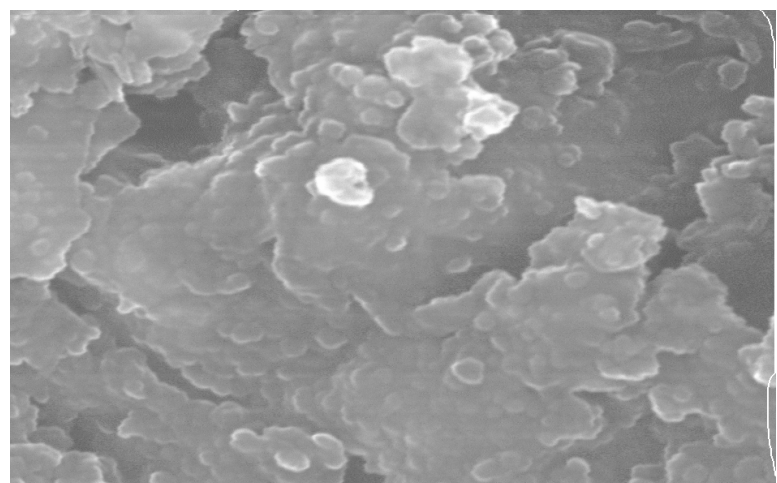
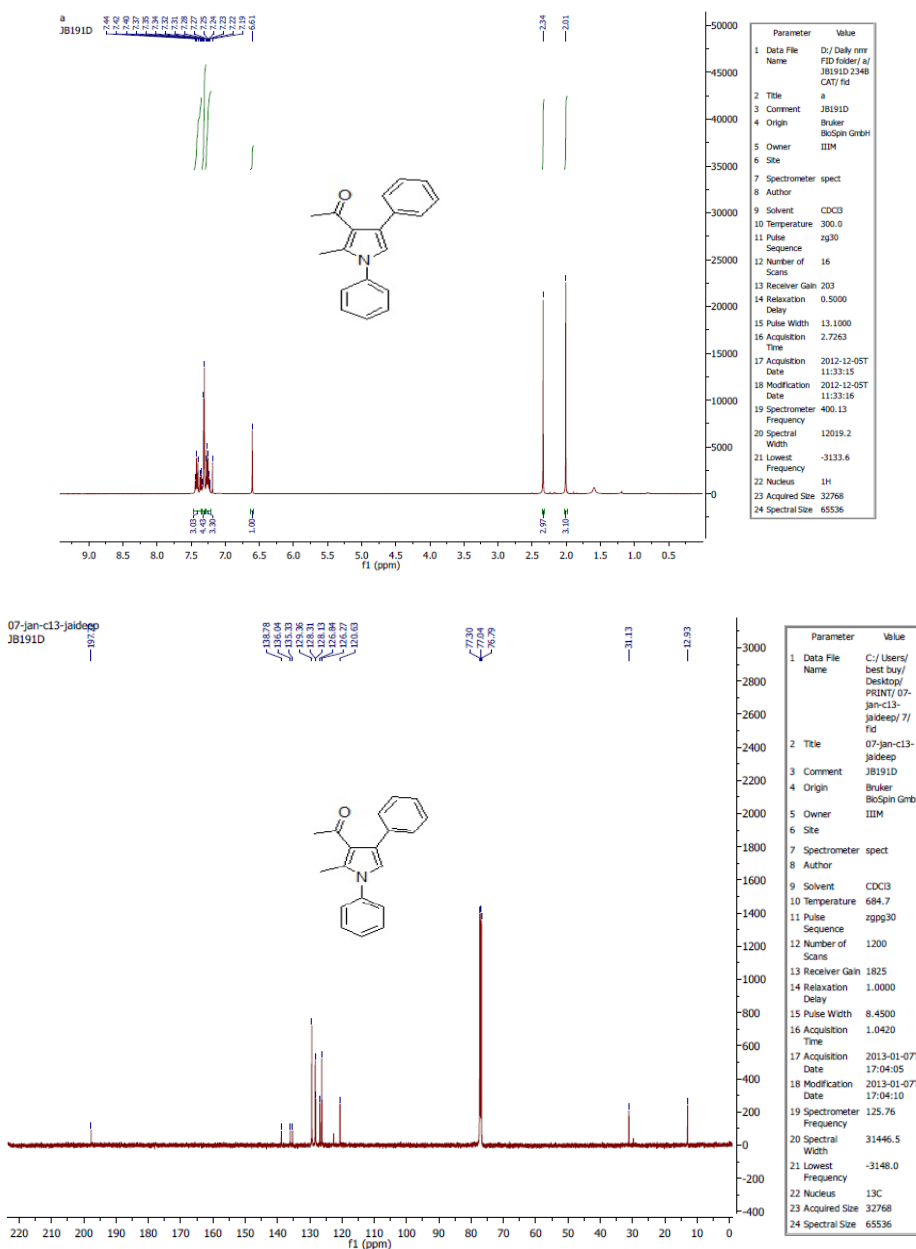
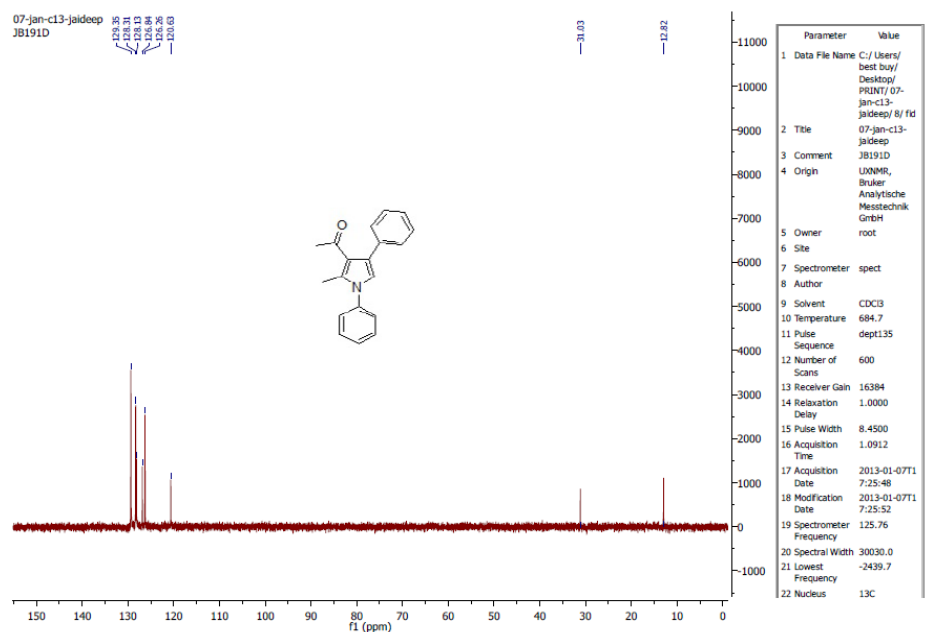


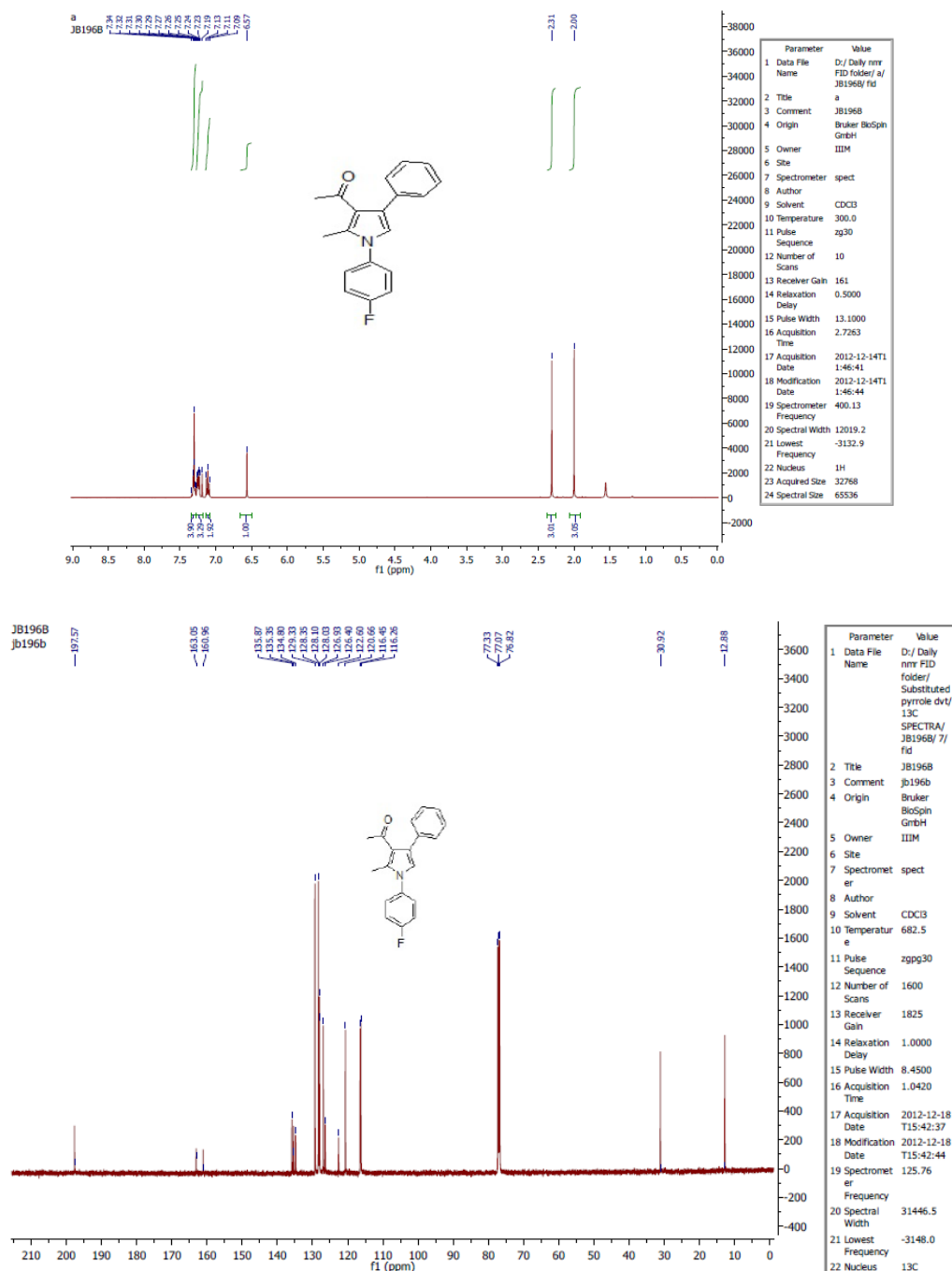
Figure S2. SEM image of Fe-PILC **B** catalyst

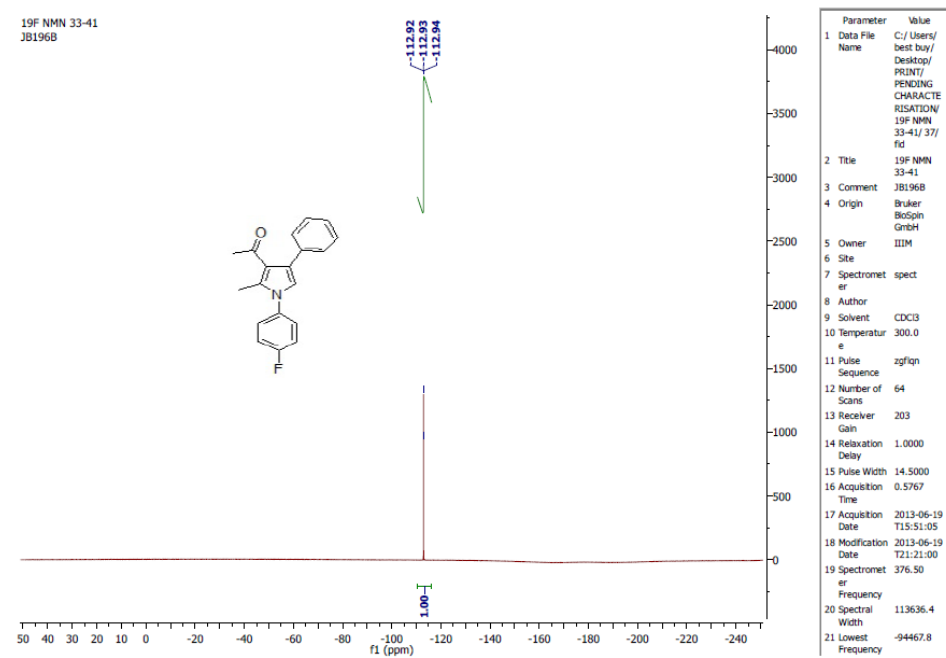
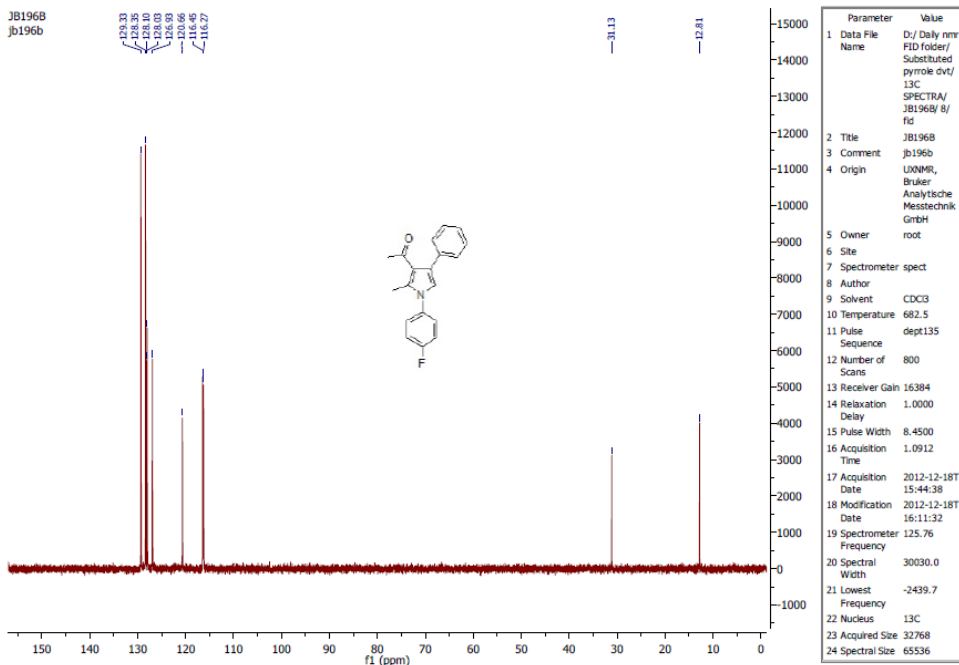
S2.a. ^1H , ^{13}C and DEPT-135 NMR of 1-(2-methyl-1,4-diphenyl-1H-pyrrol-3-yl) ethanone (**1a**):



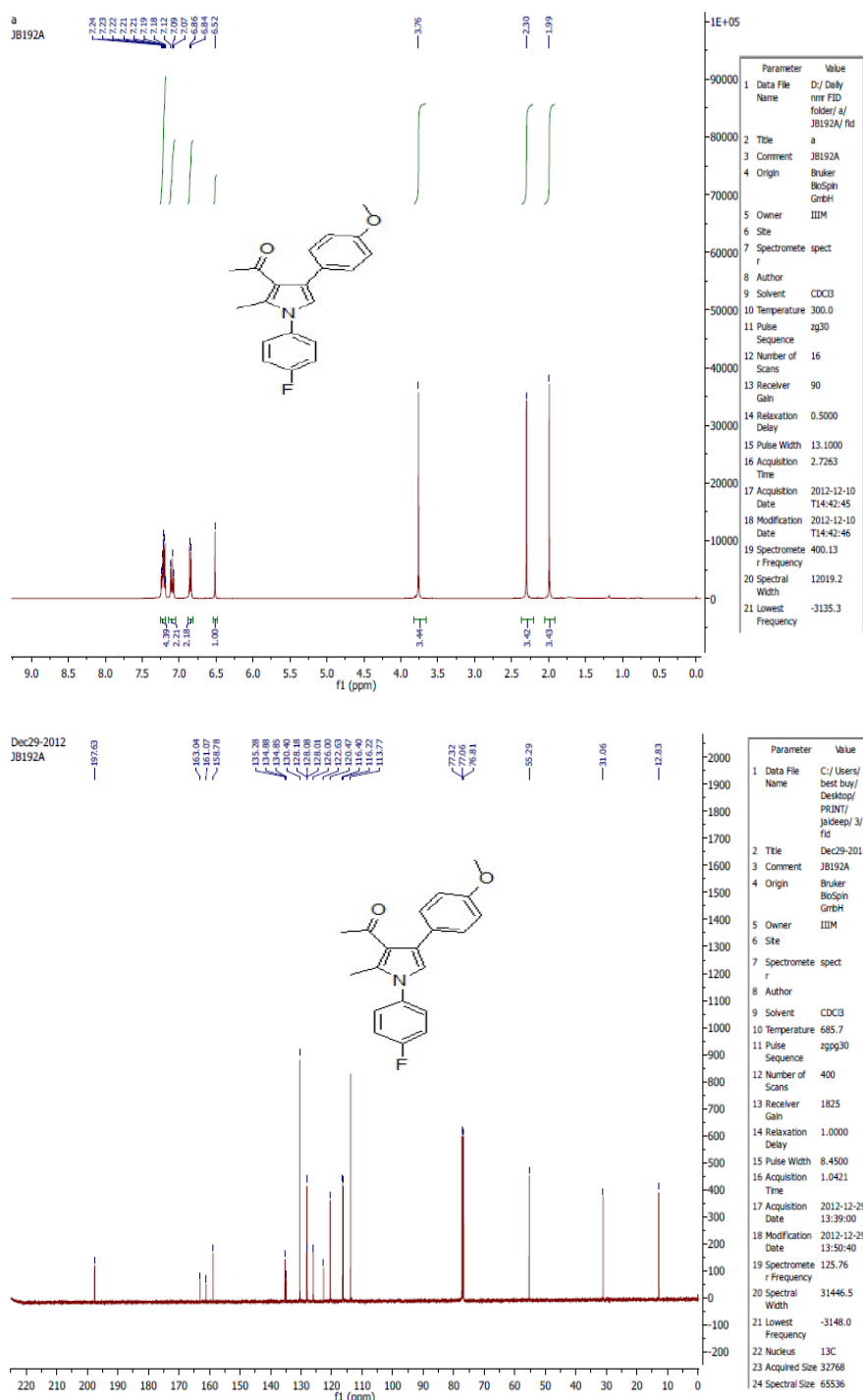


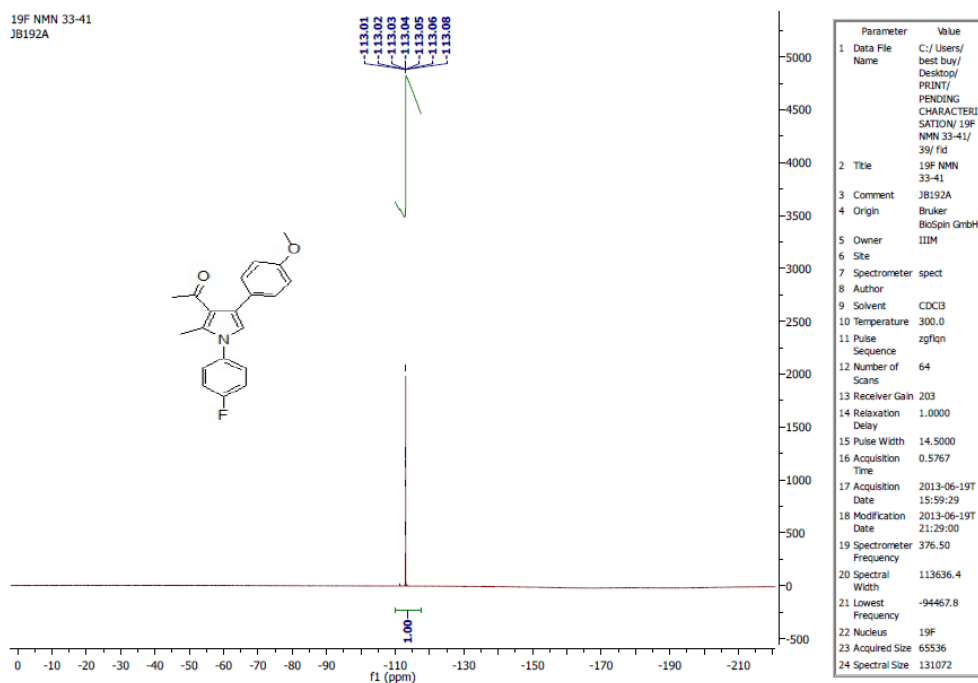
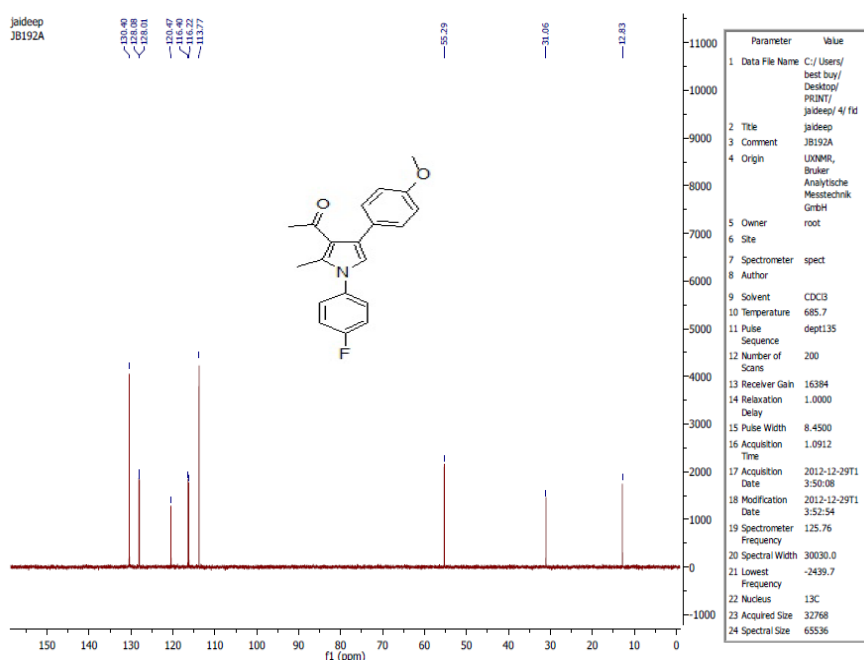
S2.b. ^1H , ^{13}C DEPT-135 NMR, ^{19}F of 1-(1-(4-fluorophenyl)-2-methyl-4-phenyl-1H-pyrrol-3-yl) ethanone (1b)



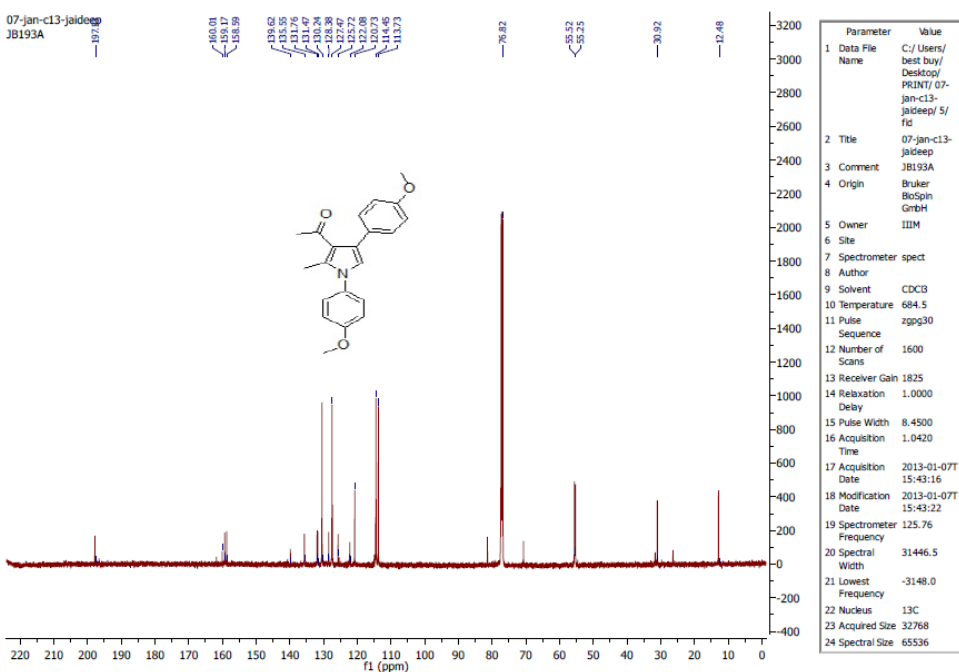
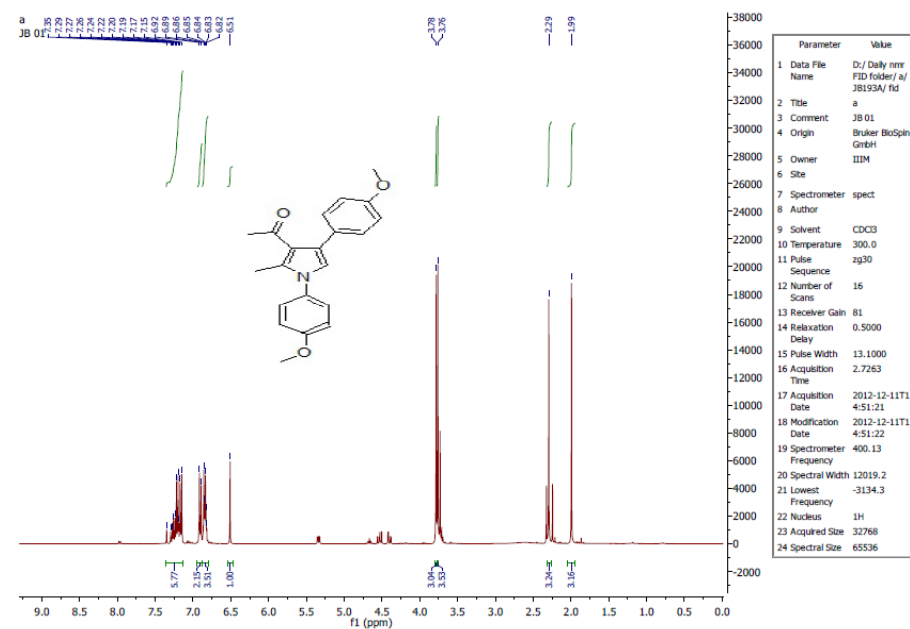


S2.c. ^1H , ^{13}C , DEPT-135 NMR and ^{19}F of 1-(1-(4-fluorophenyl)-4-(4-methoxyphenyl)-2-methyl-1H-pyrrol-3-yl)ethanone (1c)

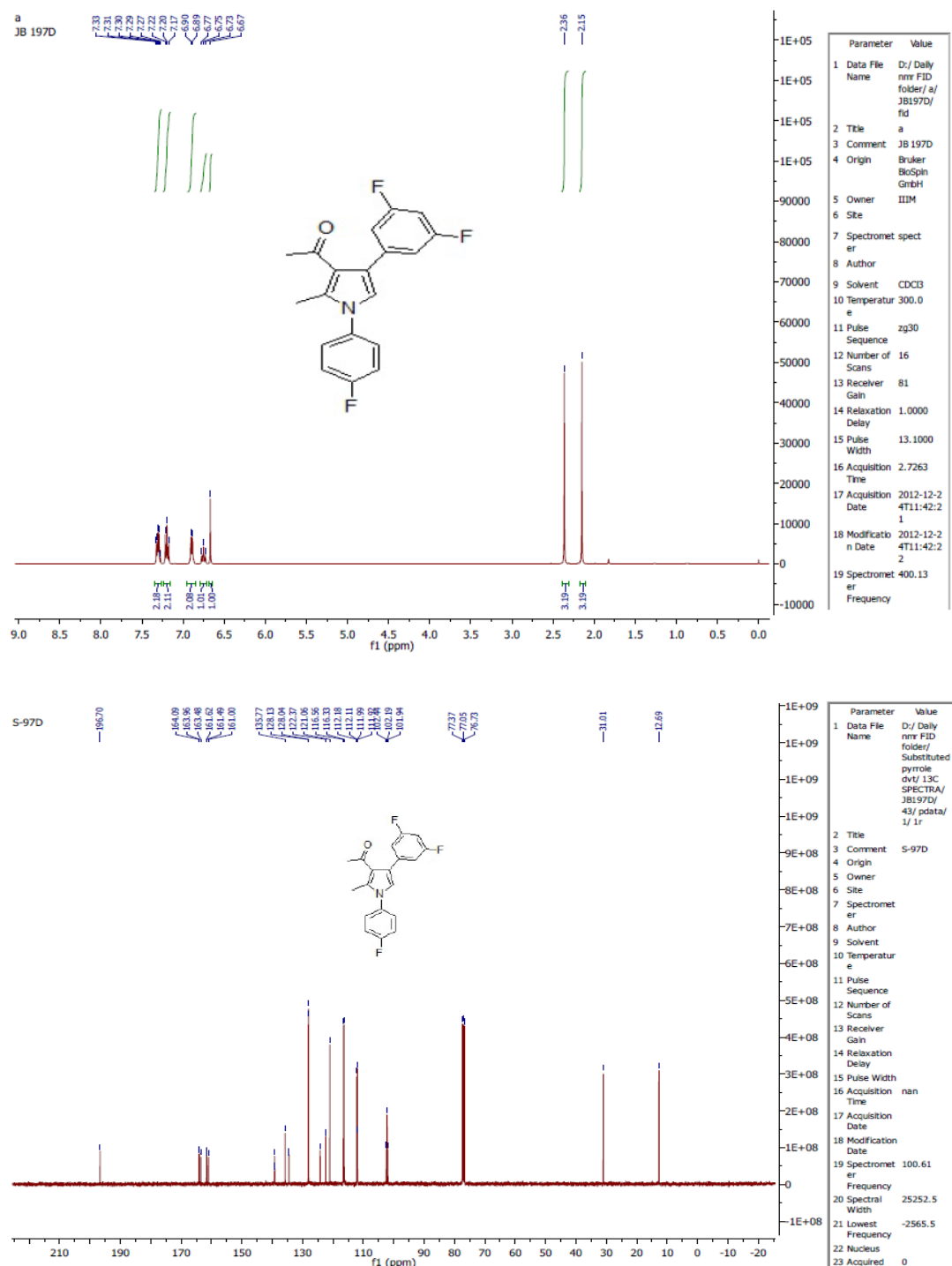


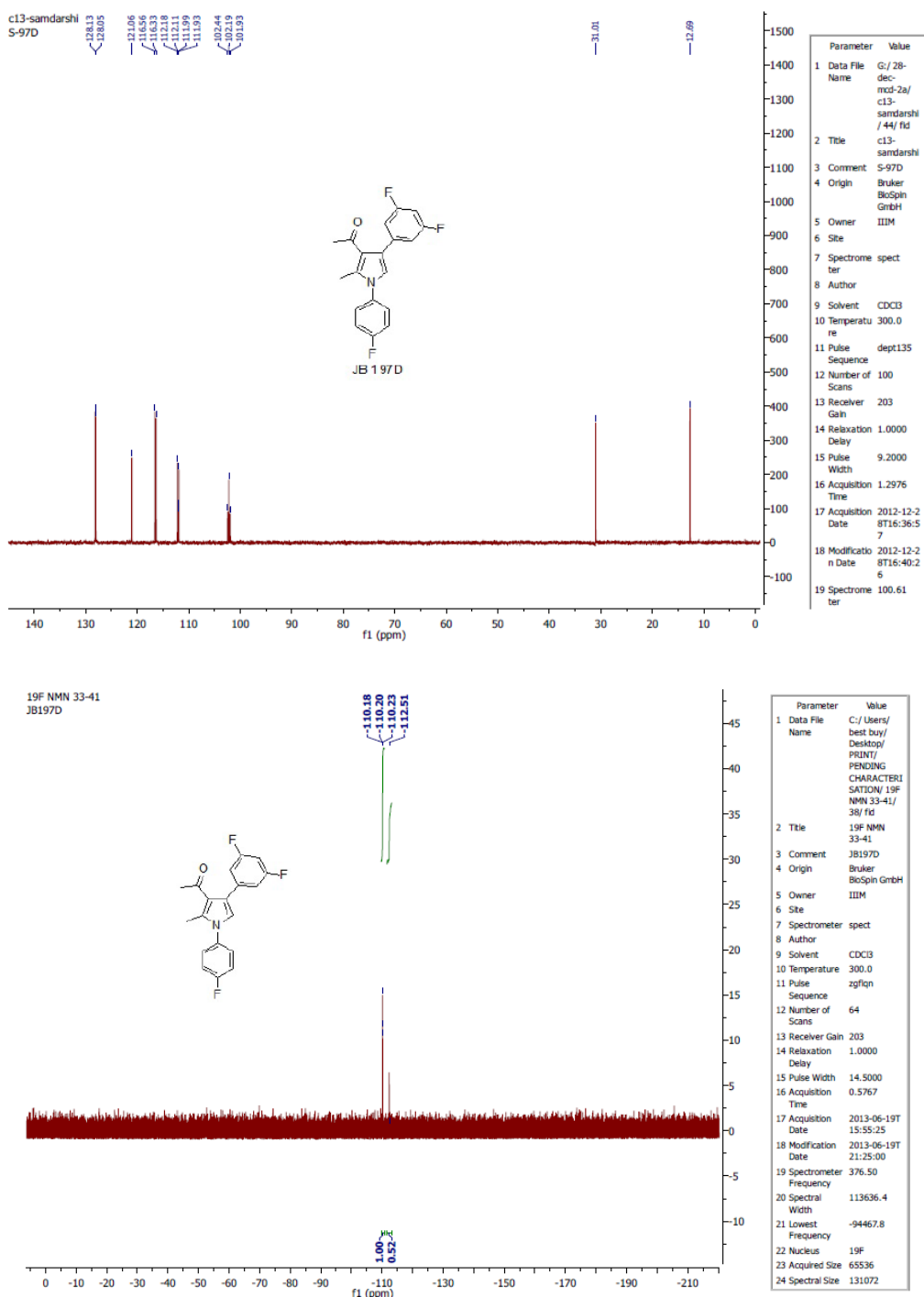


S2.d. ^1H , ^{13}C and DEPT-135 NMR of 1-(1,4-bis(4-methoxyphenyl)-2-methyl-1H-pyrrol-3-yl)ethanone (1d)

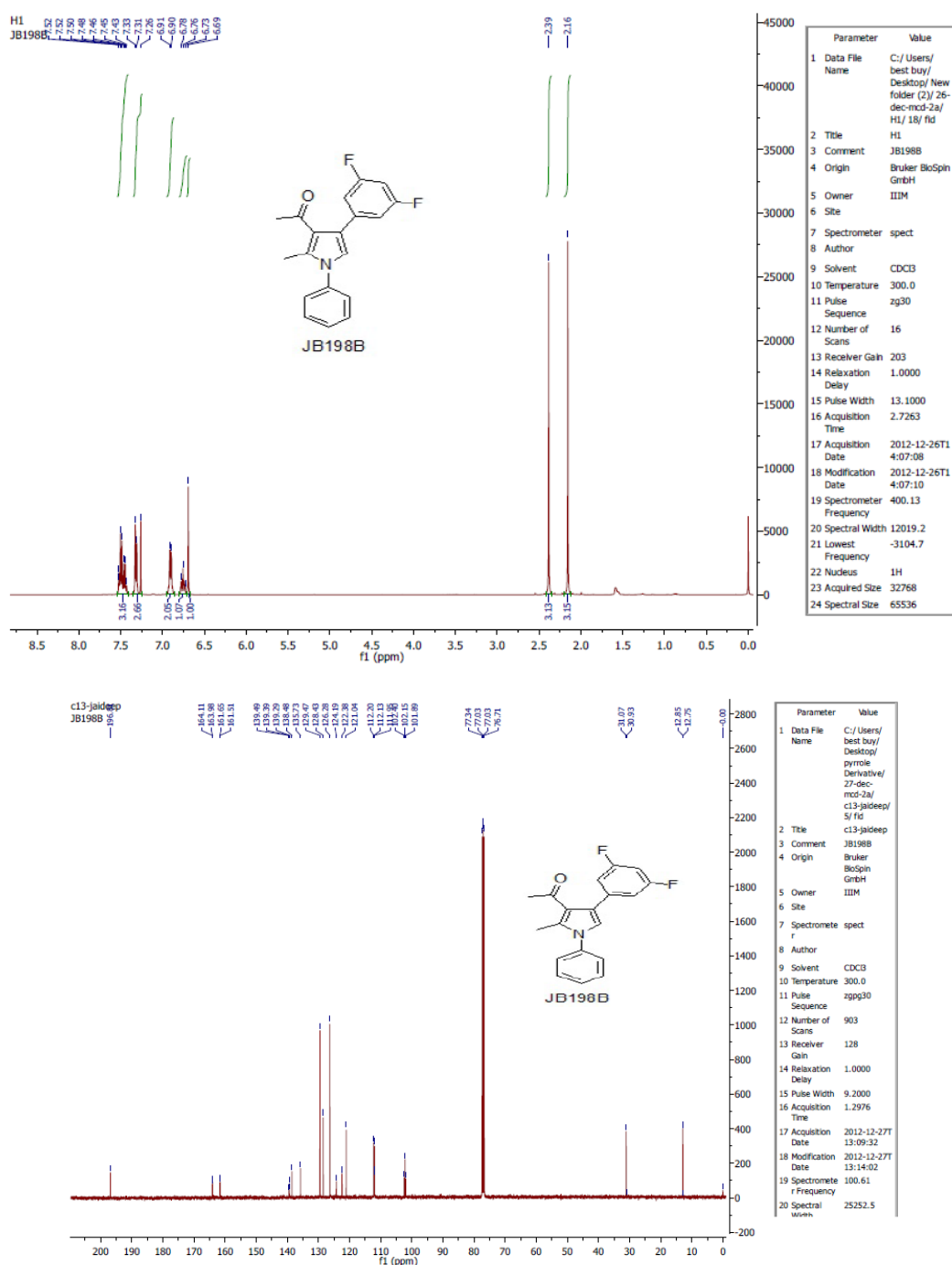


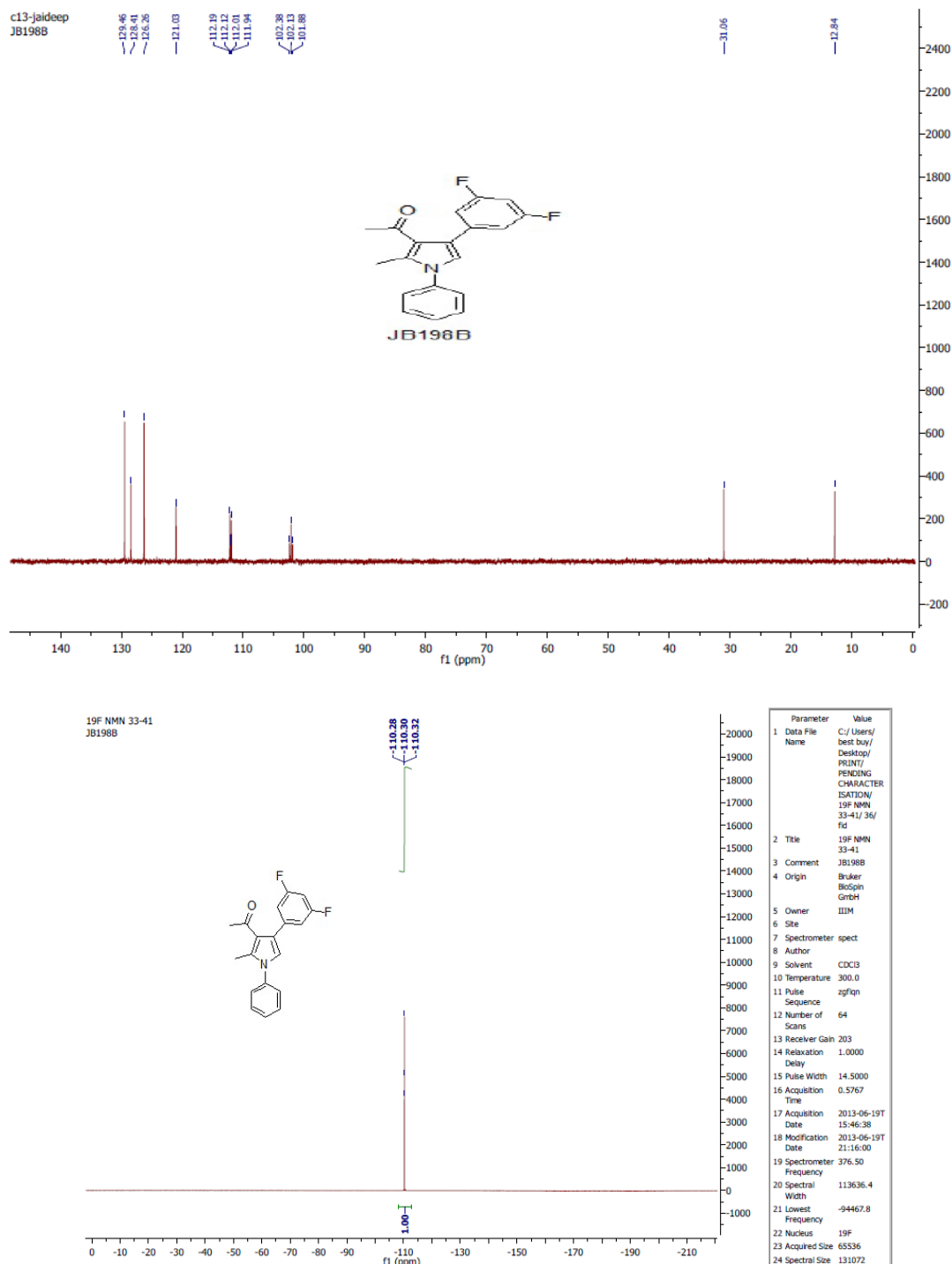
S2.e. ^1H , ^{13}C , DEPT-135 and ^{19}F NMR of 1-(4-(3,5-difluorophenyl)-1-(4-fluorophenyl)-2-methyl-1H-pyrrol-3-yl)ethanone (1e)



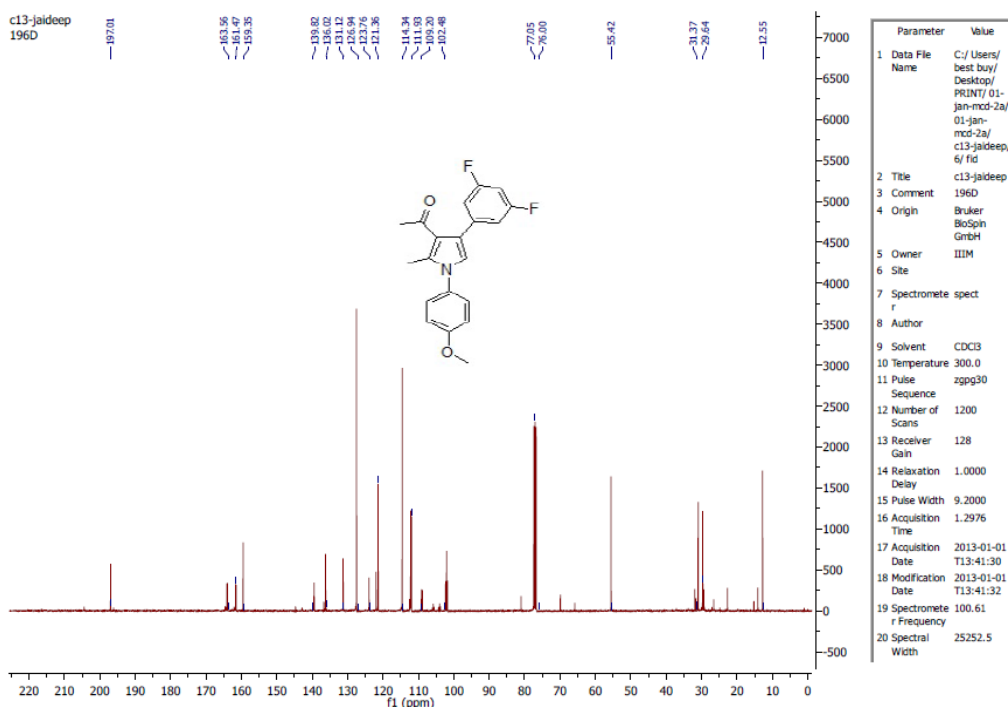
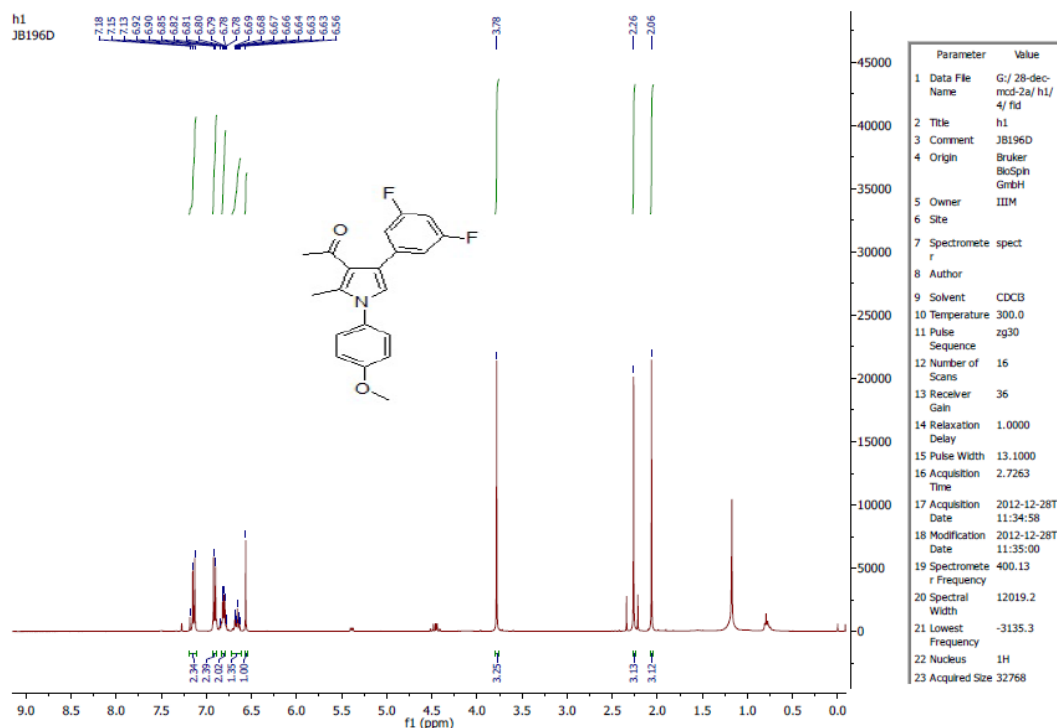


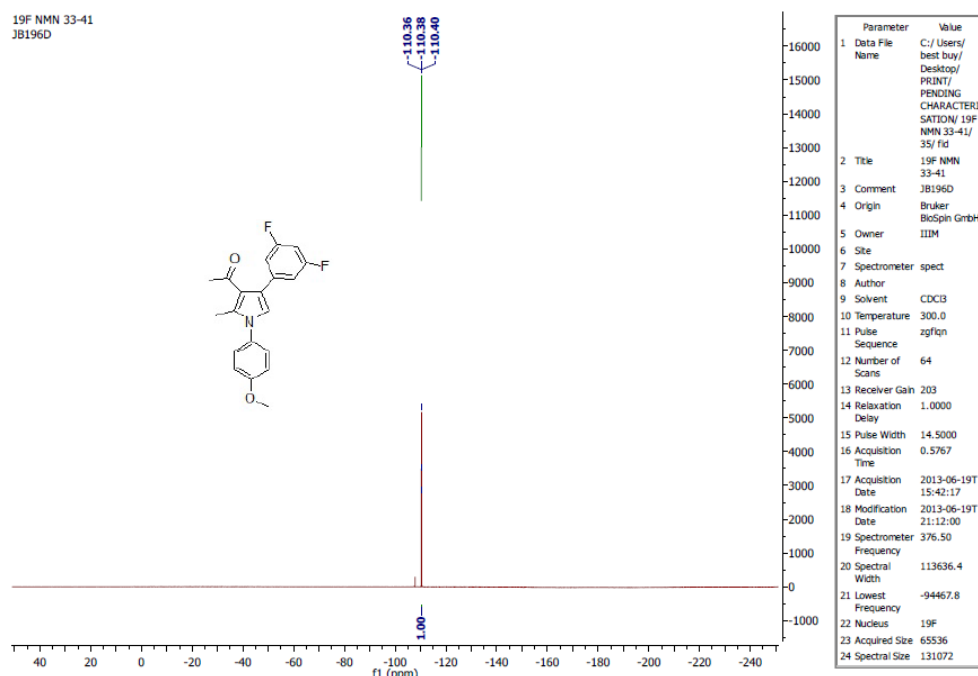
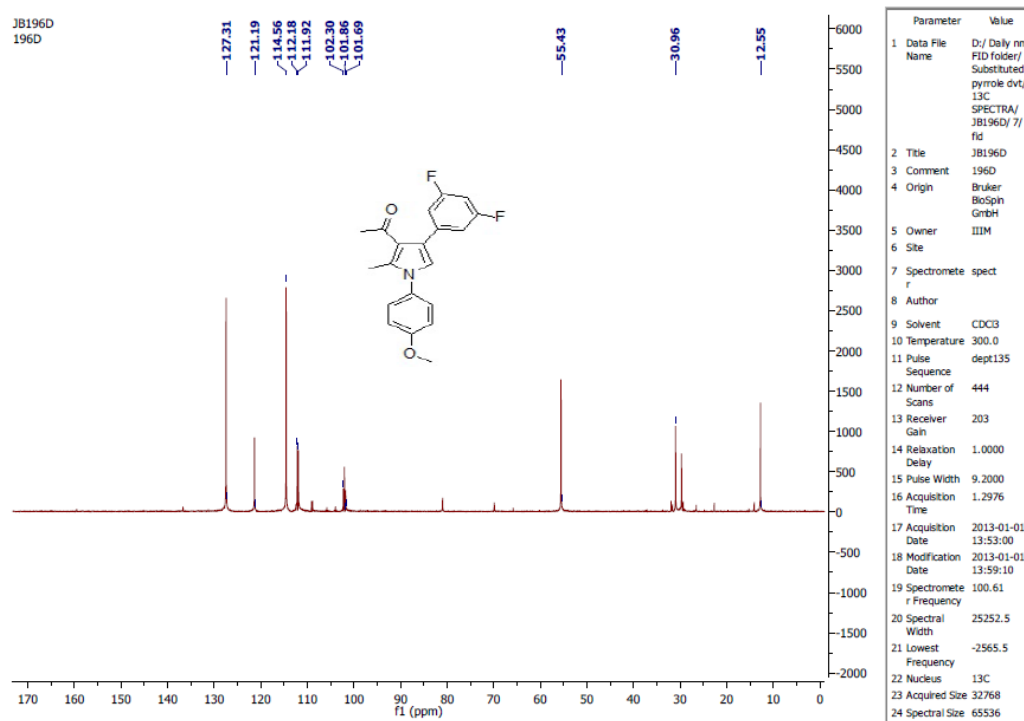
S2.f. ^1H , ^{13}C ,DEPT-135 and ^{19}F NMR of 1-(4-(3,5-difluorophenyl)-2-methyl-1-phenyl-1H-pyrrol-3-yl)ethanone (1f)



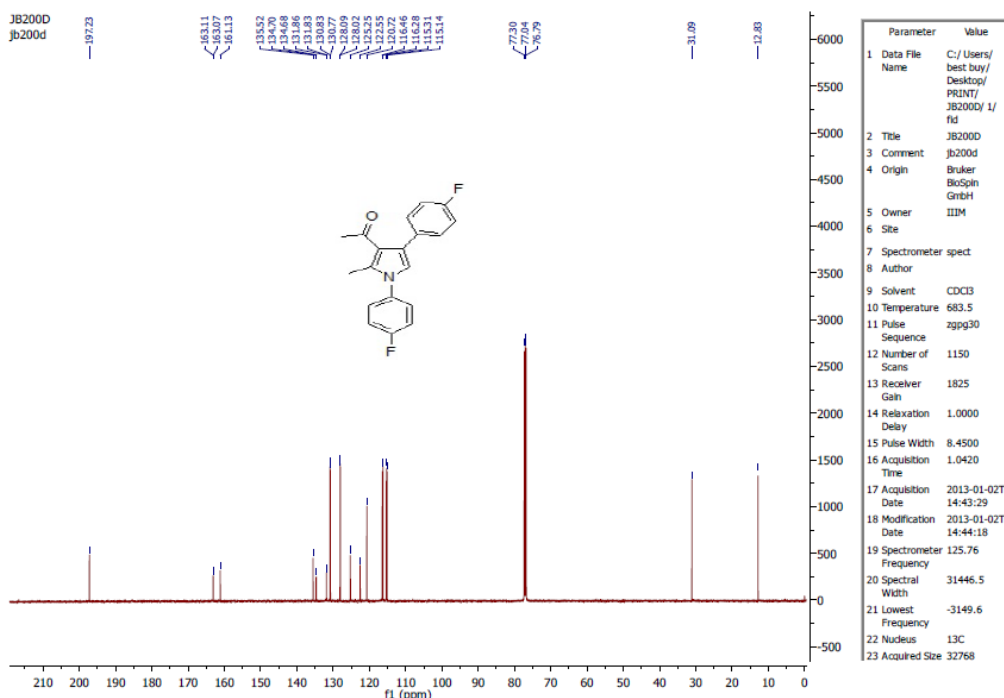
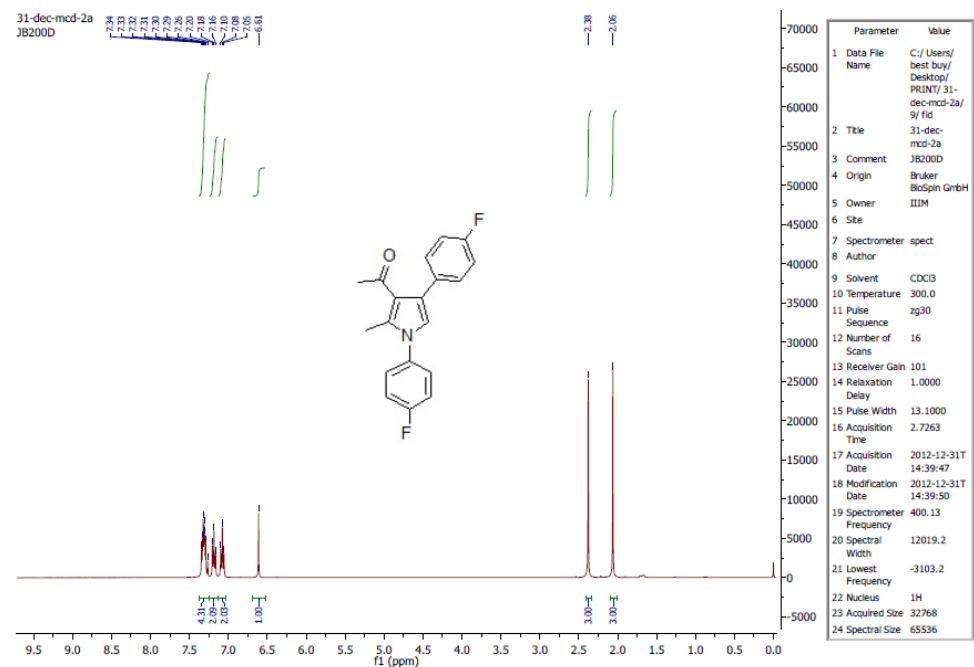


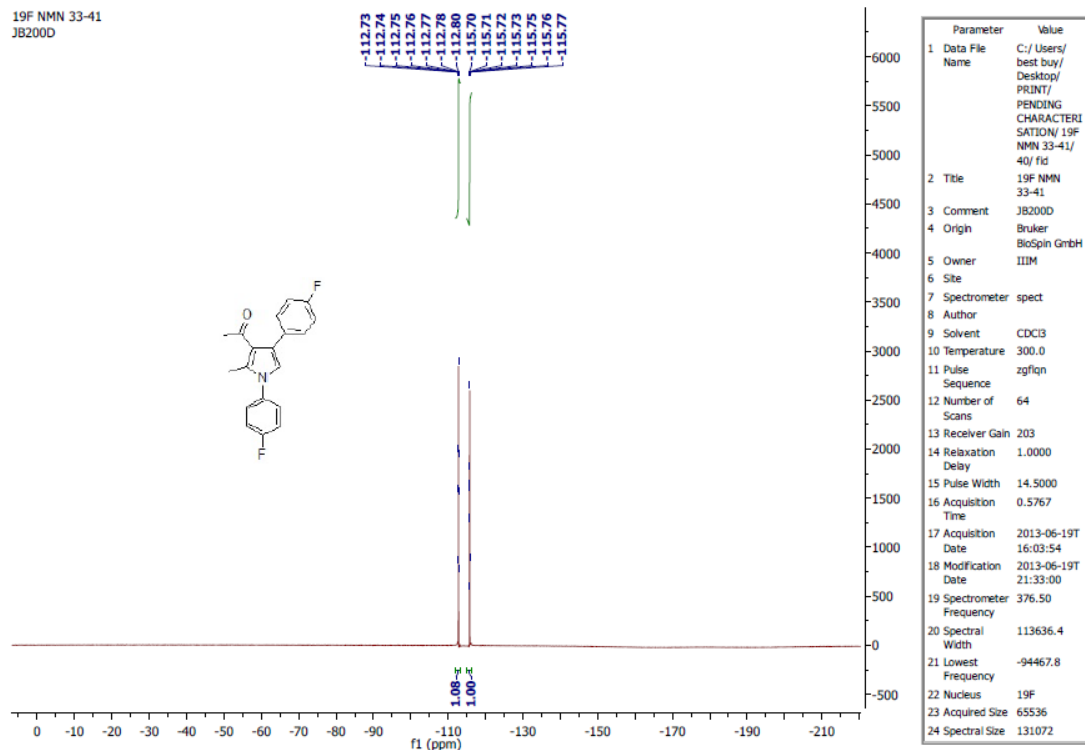
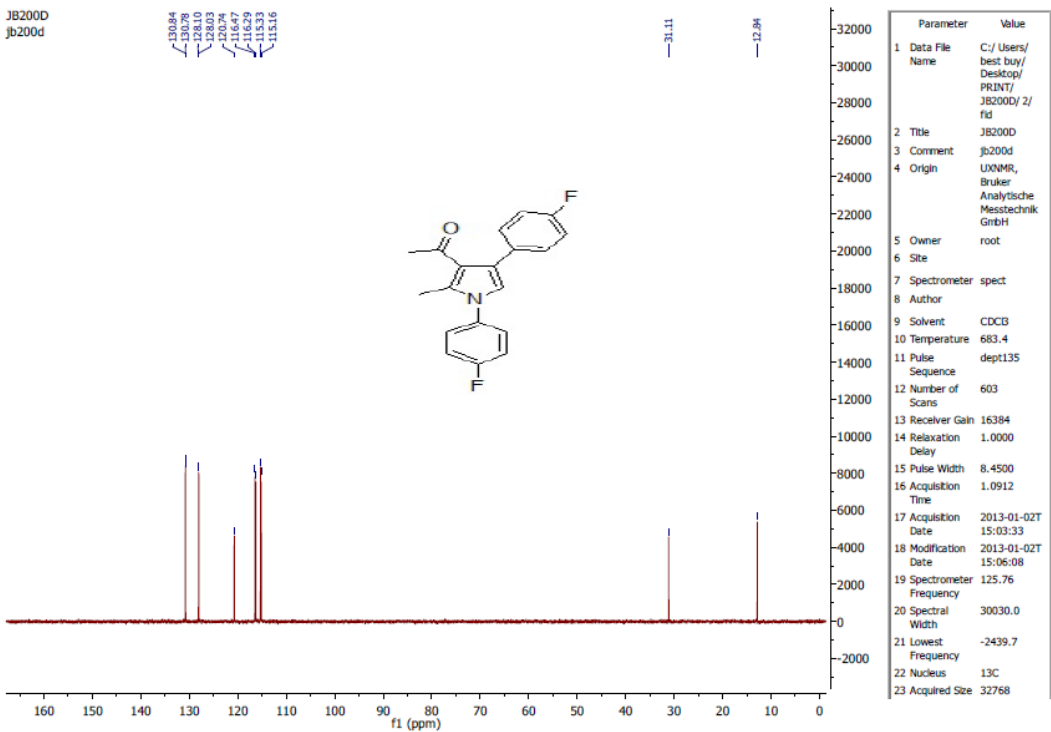
S2.g. ^1H , ^{13}C ,DEPT-135 and ^{19}F NMR of 1-(4-(3,5-difluorophenyl)-1-(4-methoxyphenyl)-2-methyl-1H-pyrrol-3-yl)ethanone (1g)



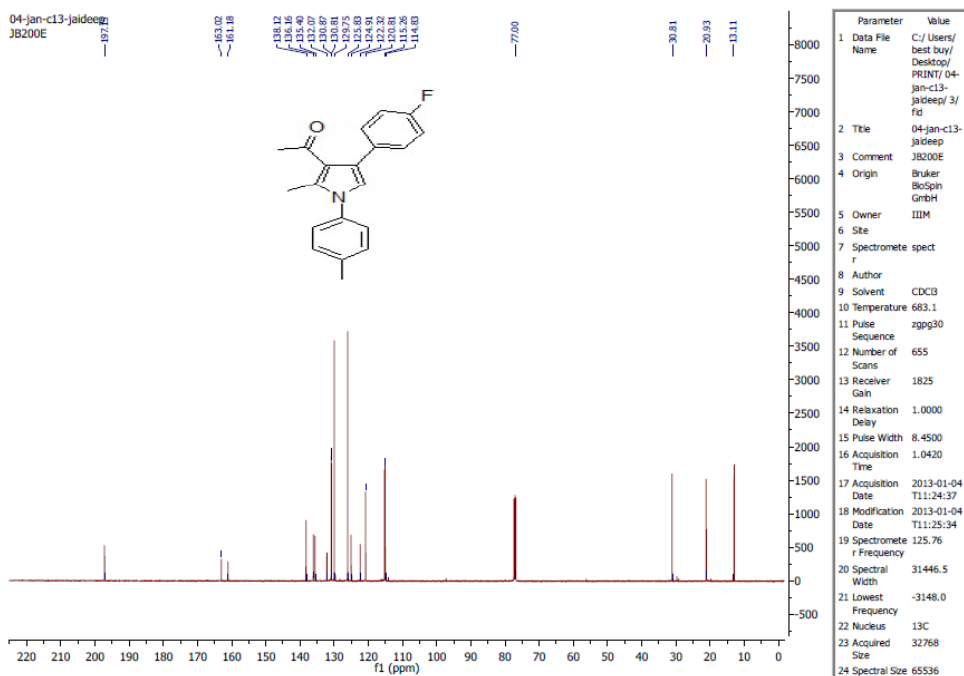
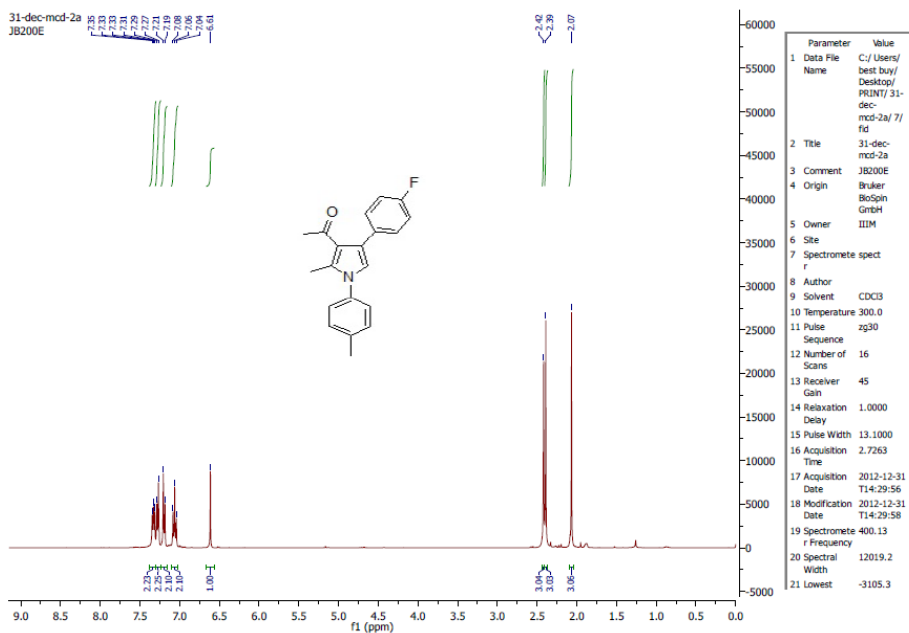


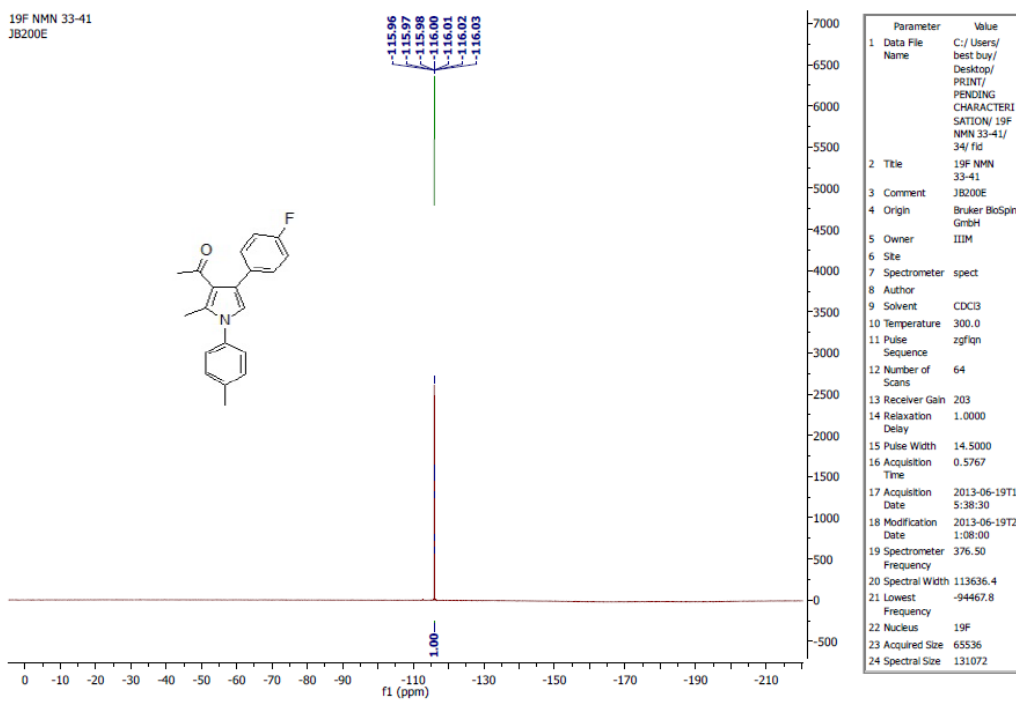
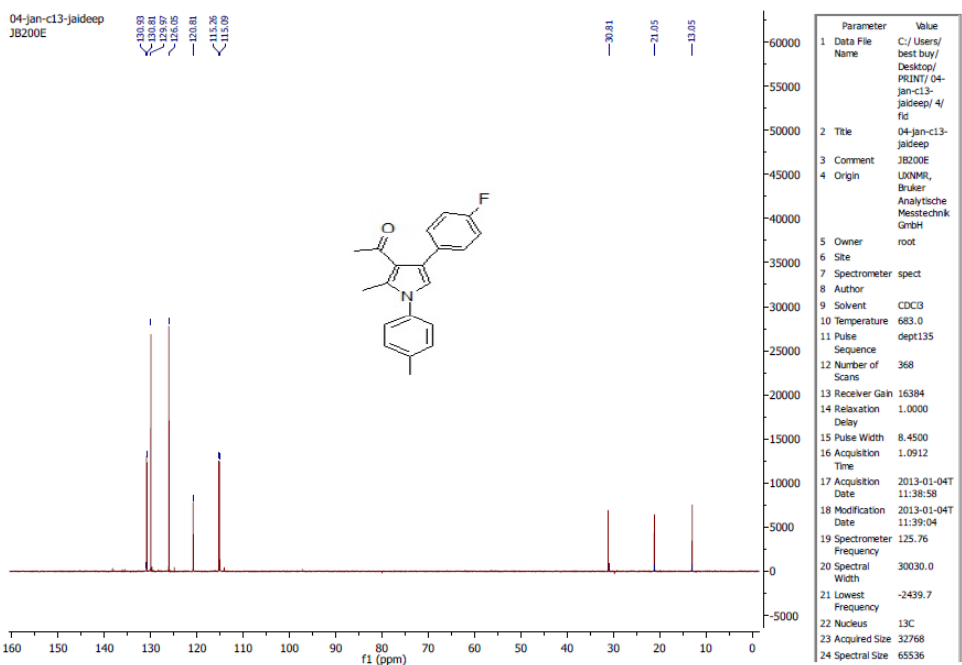
S2.h. ^1H , ^{13}C , DEPT-135 and ^{19}F NMR of 1-(1,4-bis(4-fluorophenyl)-2-methyl-1H-pyrrol-3-yl)ethanone (1h)



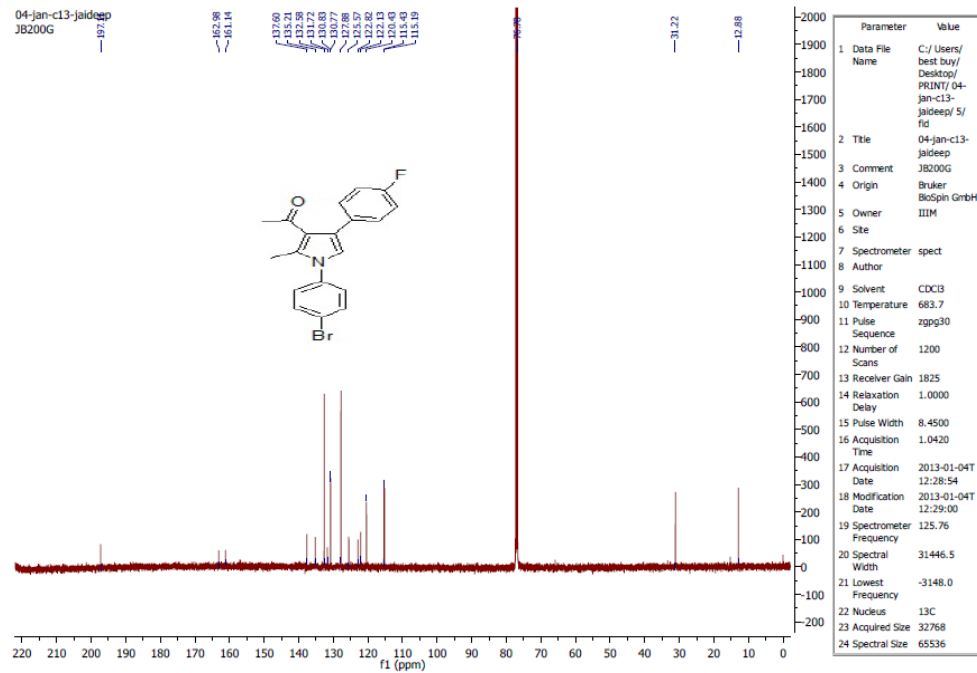
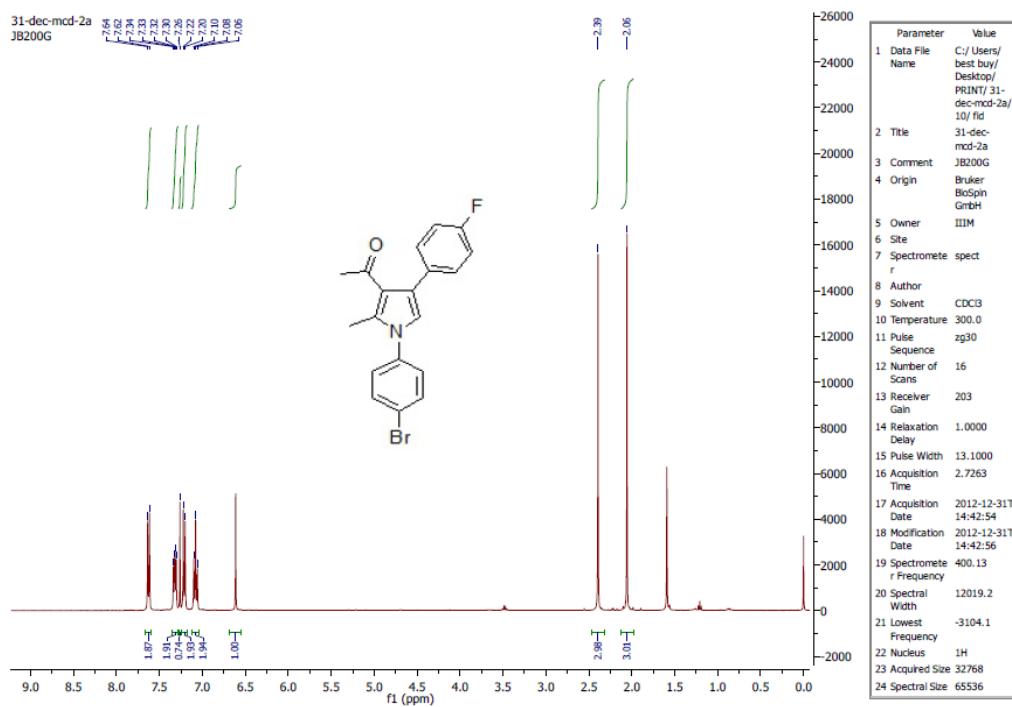


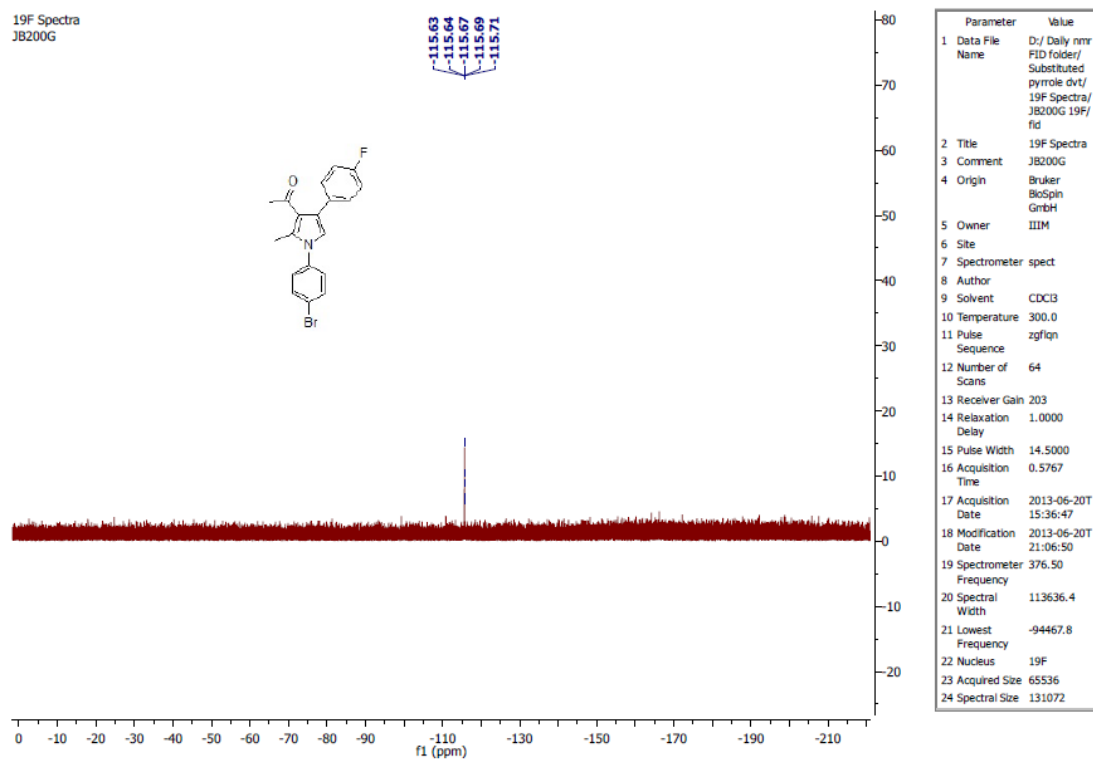
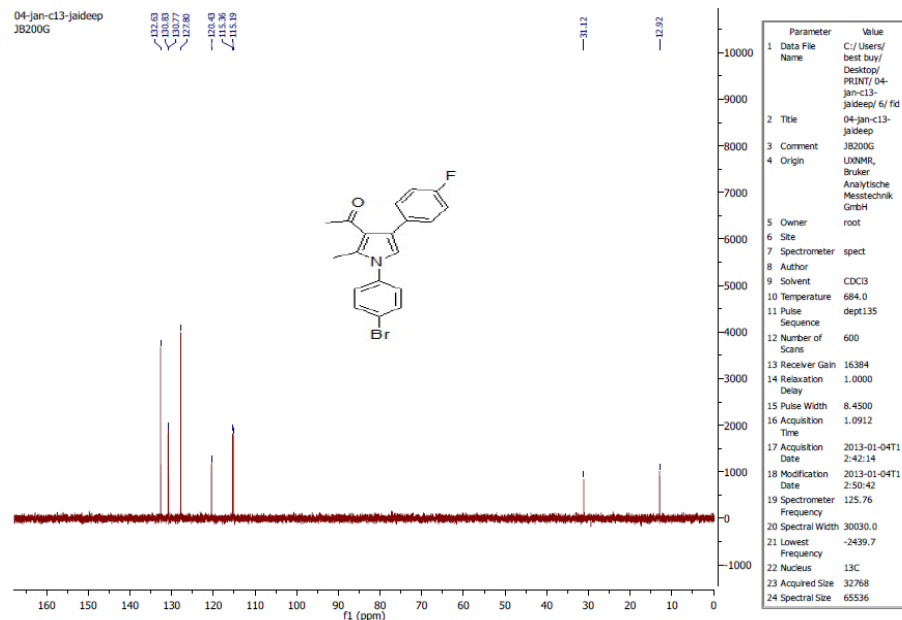
S2.i. ^1H , ^{13}C , DEPT-135 and ^{19}F NMR of 1-(4-(4-fluorophenyl)-2-methyl-1-p-tolyl-1H-pyrrol-3-yl)ethanone (1i)



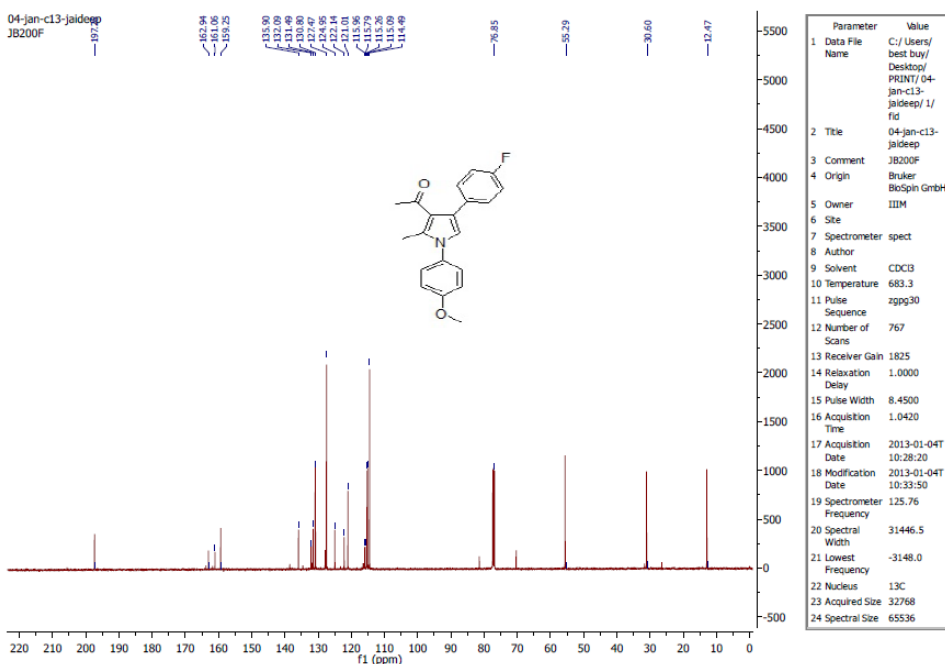
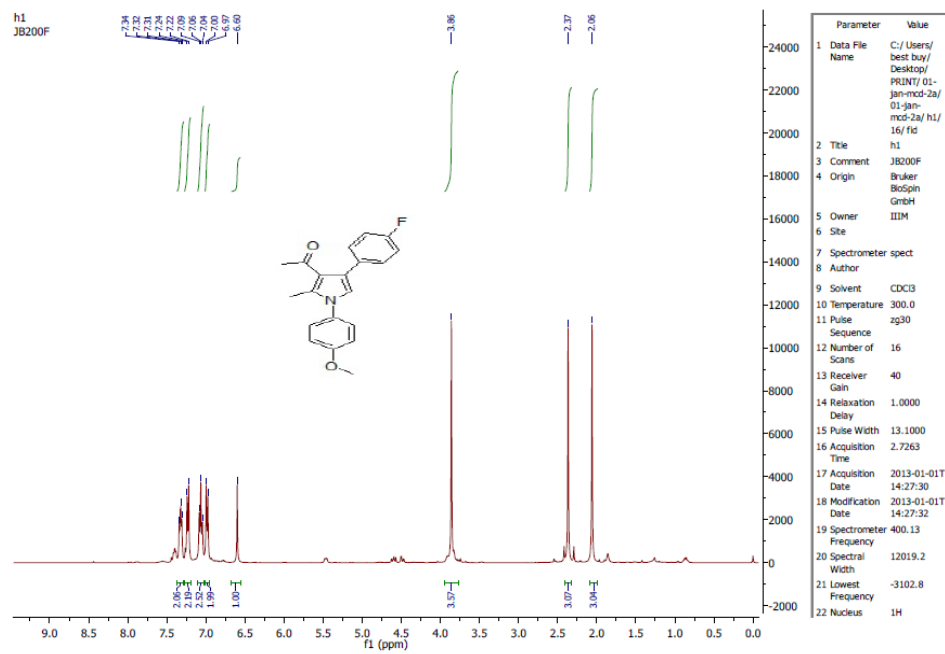


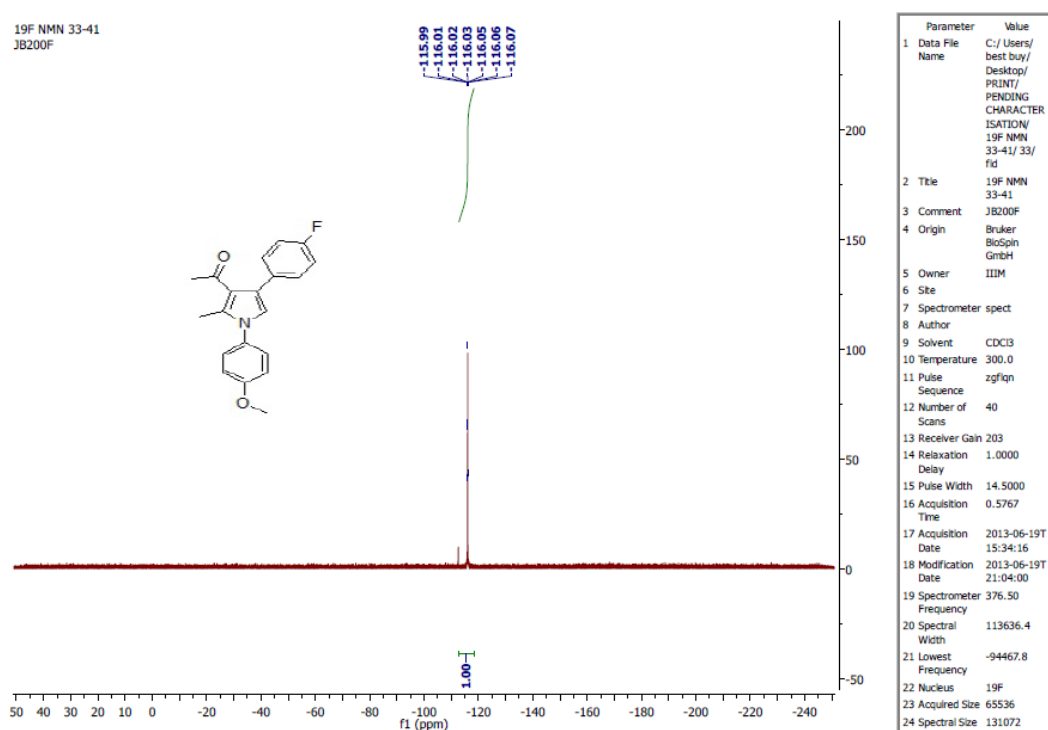
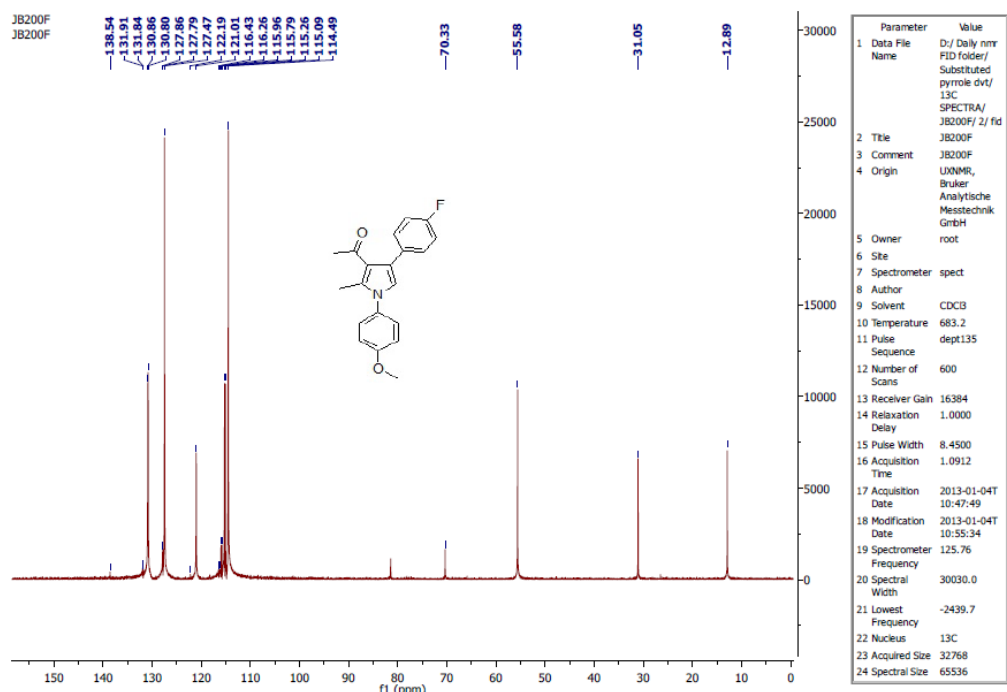
S2.j. ^1H , ^{13}C , DEPT-135 and ^{19}F NMR of 1-(1-(4-bromophenyl)-4-(4-fluorophenyl)-2-methyl-1H-pyrrol-3-yl)ethanone (1j)



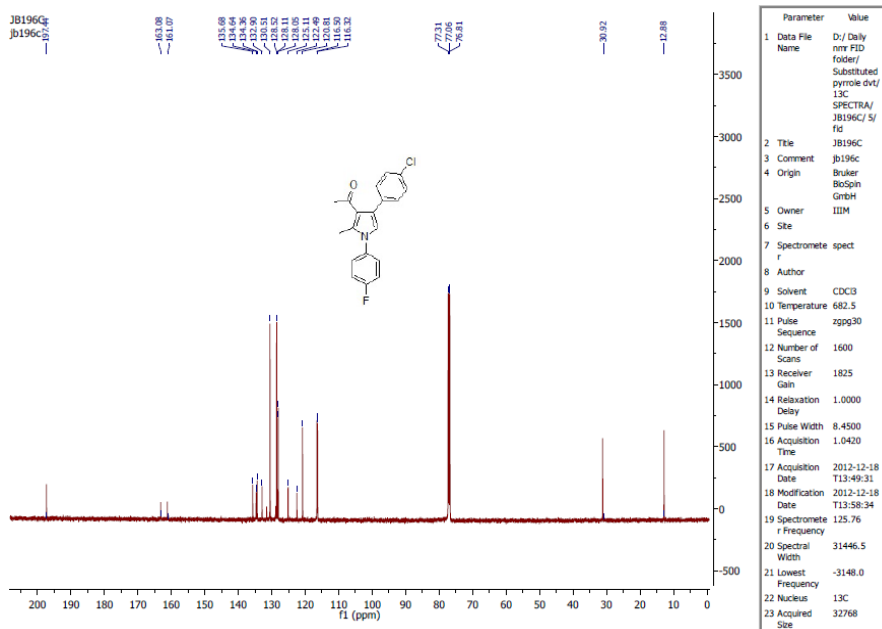
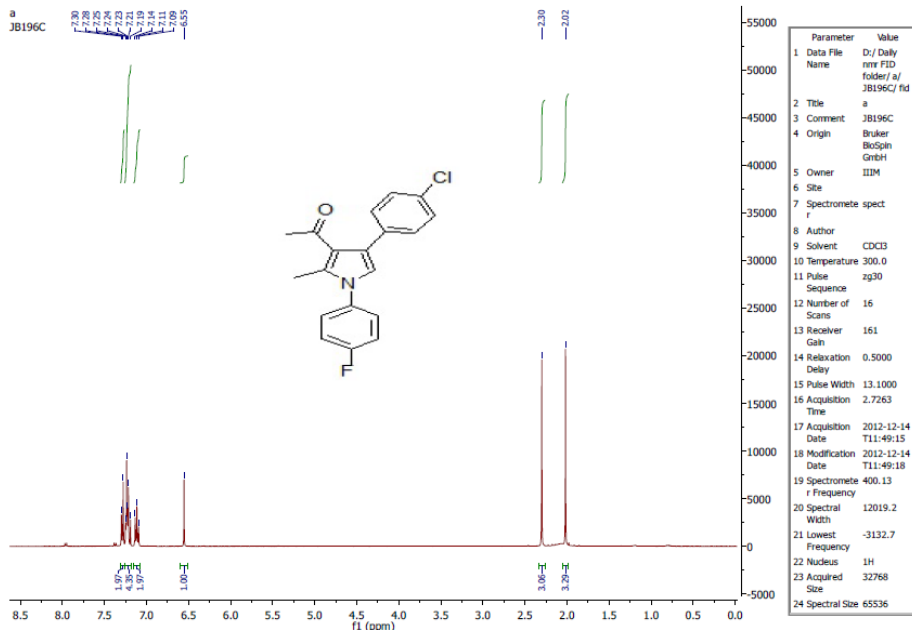


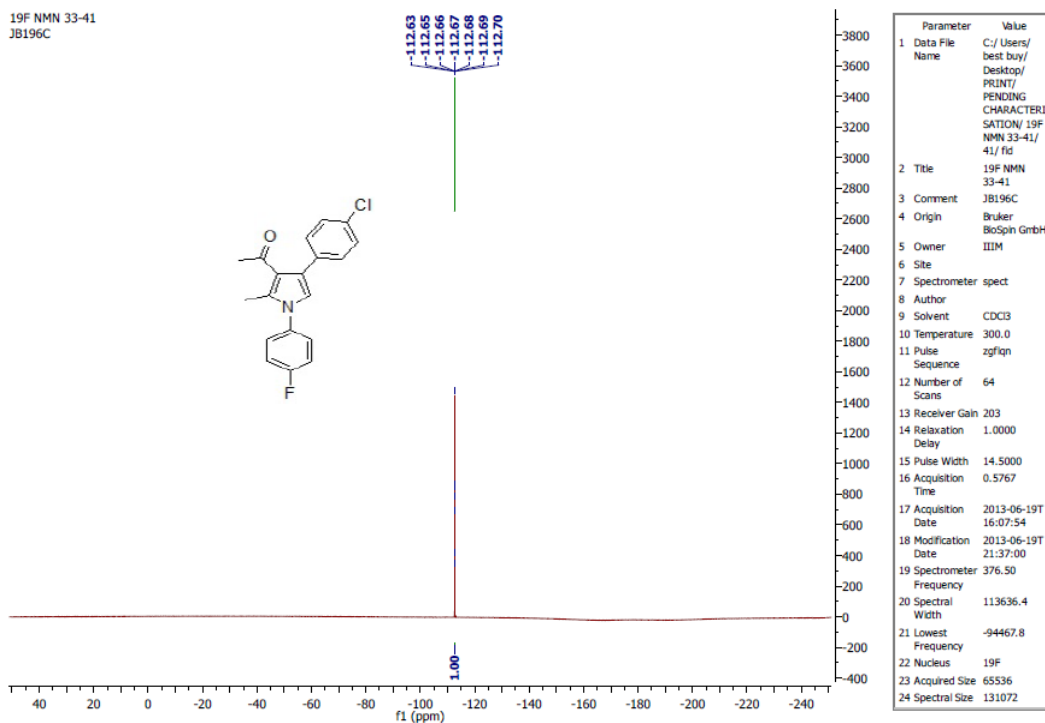
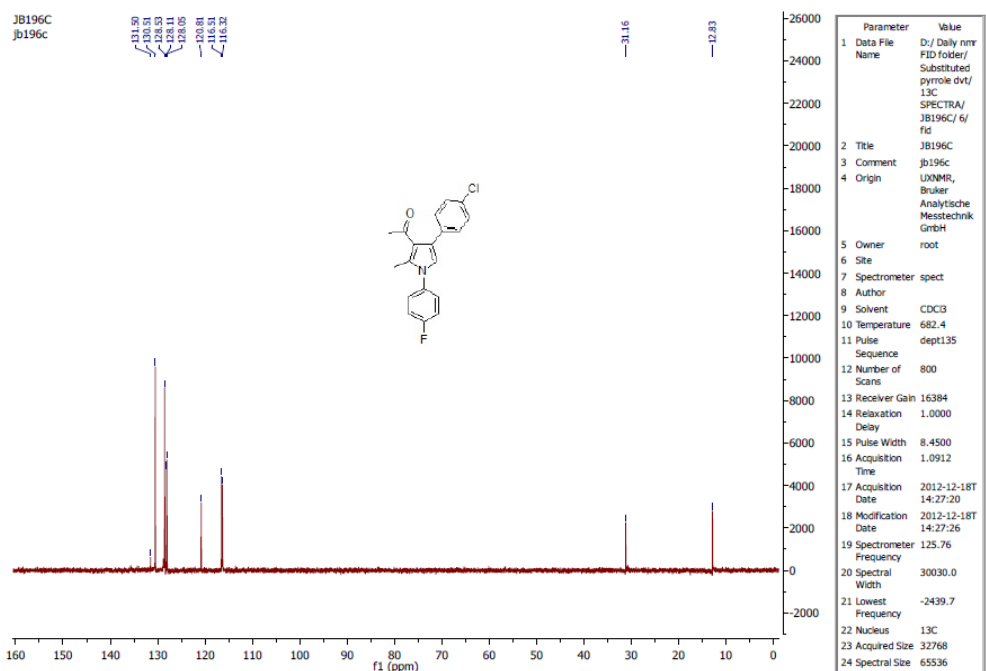
S2.k. ^1H , ^{13}C ,DEPT-135 and ^{19}F NMR of 1-(4-(4-fluorophenyl)-1-(4-methoxyphenyl)-2-methyl-1H-pyrrol-3-yl)ethanone (1k)



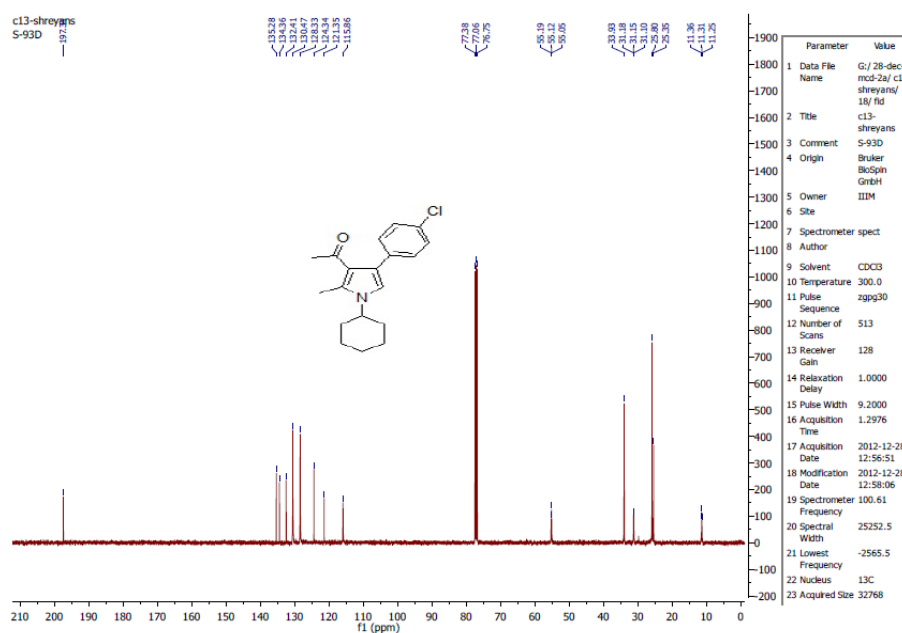
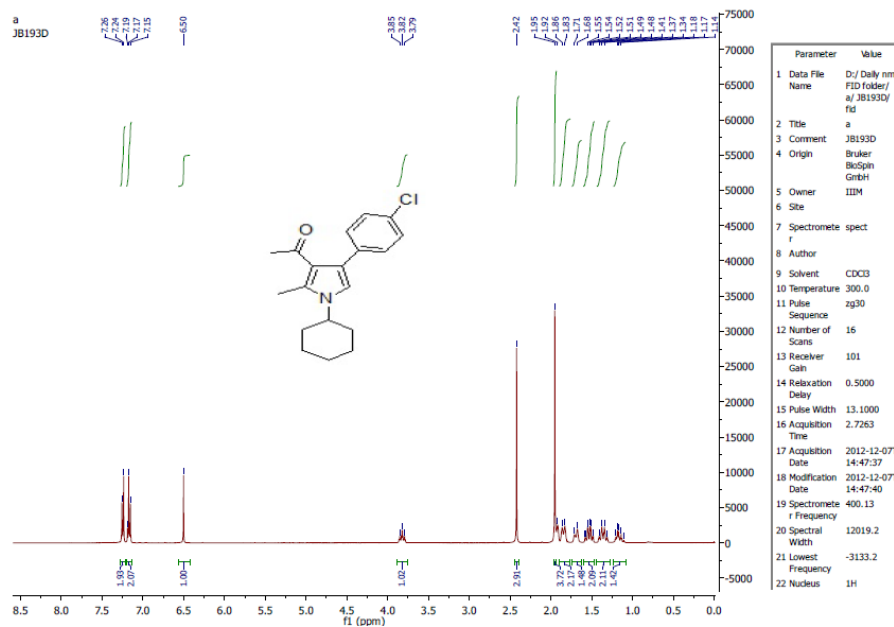


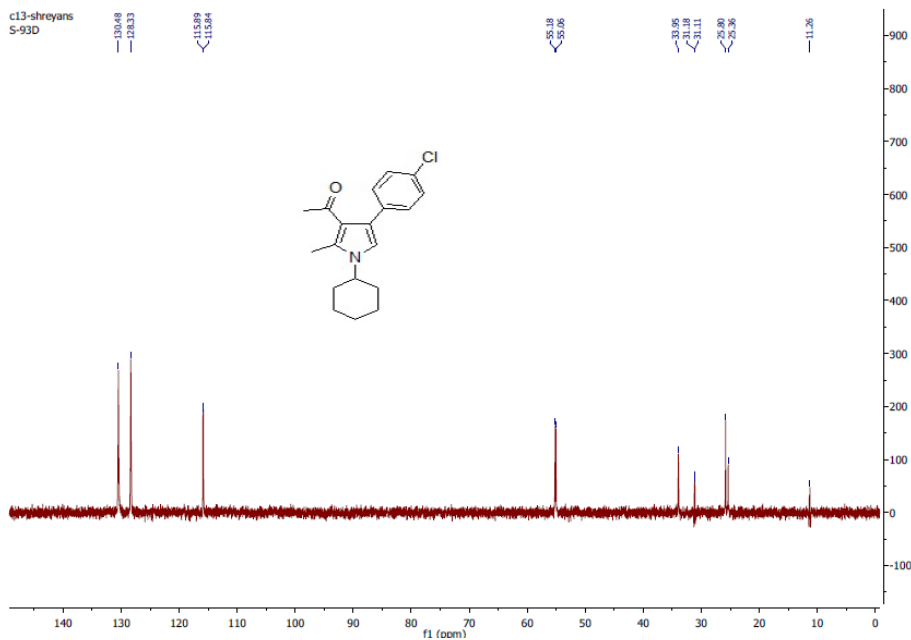
S2.l. ^1H , ^{13}C , DEPT-135 and ^{19}F NMR of 1-(4-(4-chlorophenyl)-1-(4-fluorophenyl)-2-methyl-1H-pyrrol-3-yl)ethanone (1l)



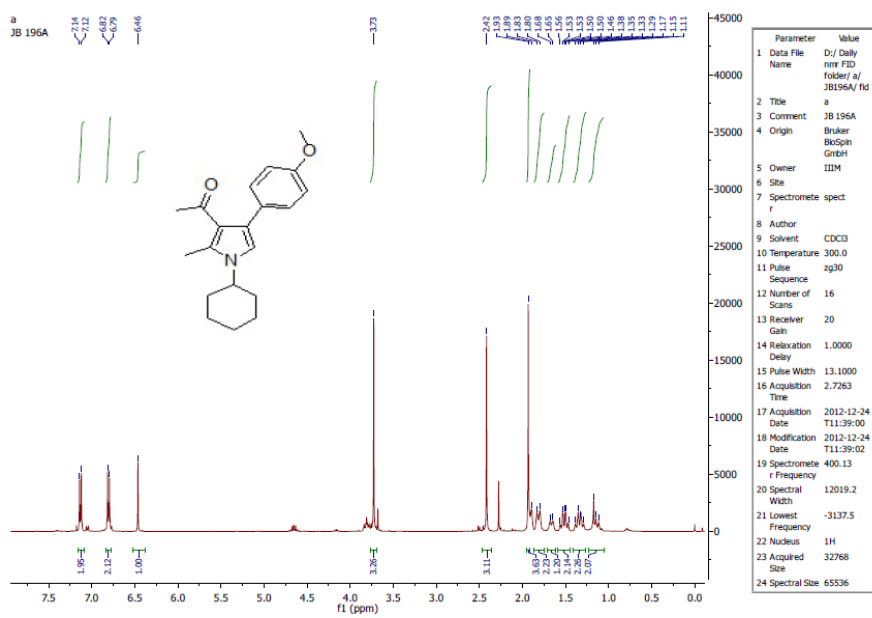


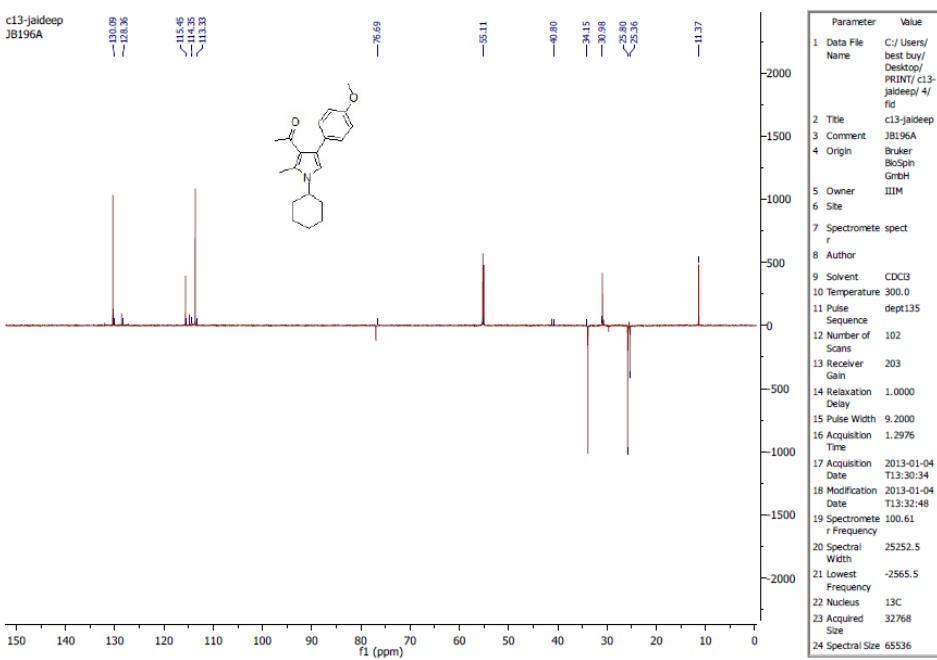
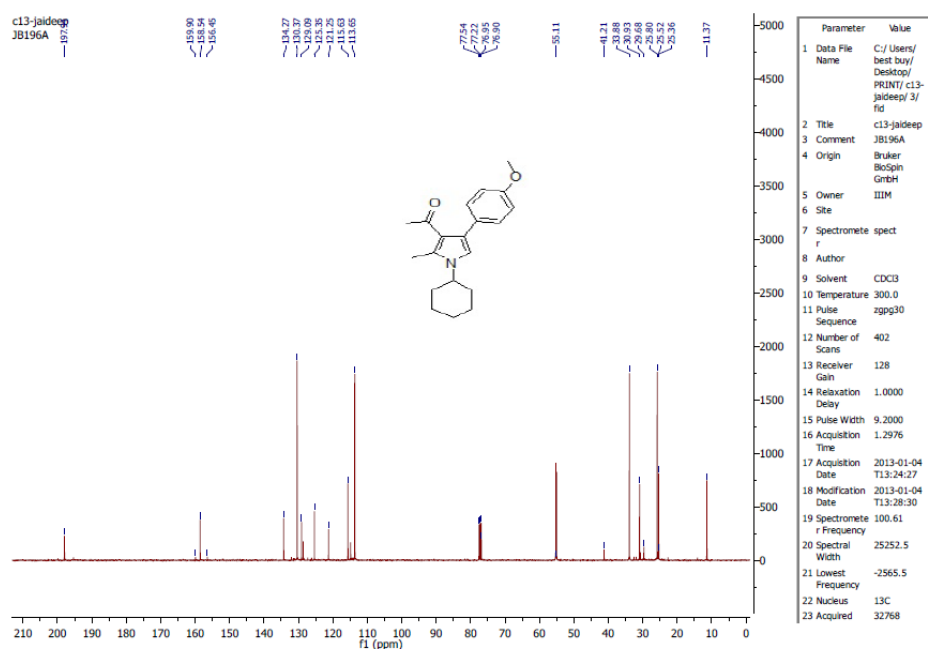
S2.m. ^1H , ^{13}C and DEPT-135 NMR of 1-(4-(4-chlorophenyl)-1-cyclohexyl-2-methyl-1H-pyrrol-3-yl)ethanone (1m)



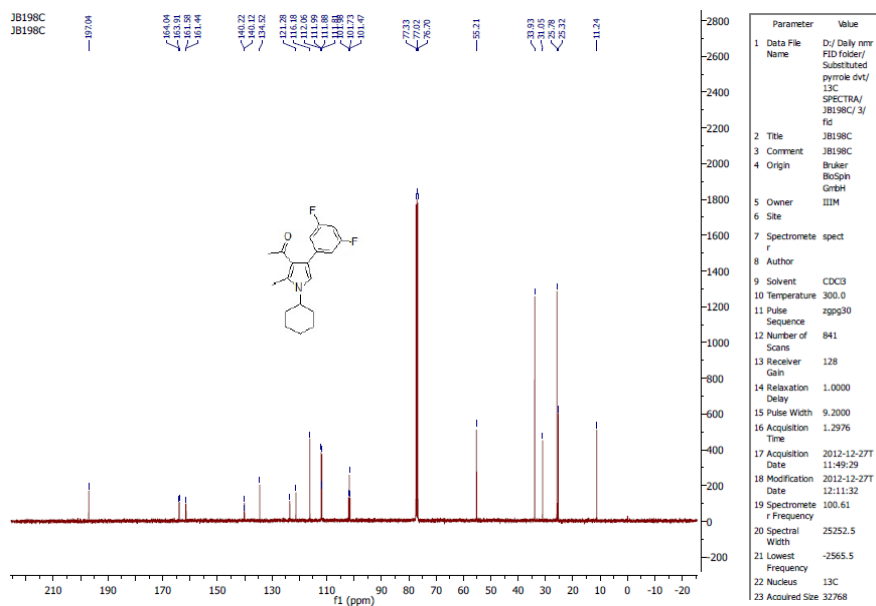
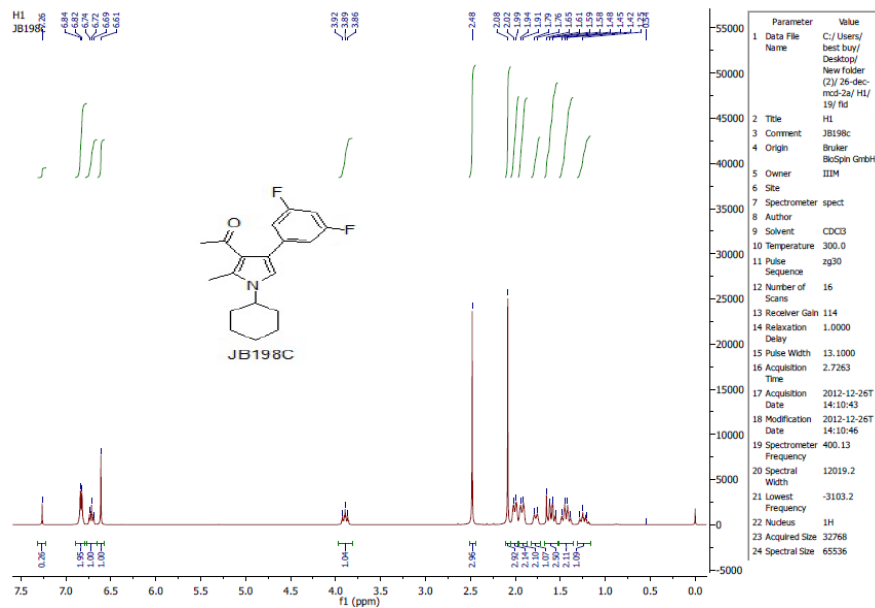


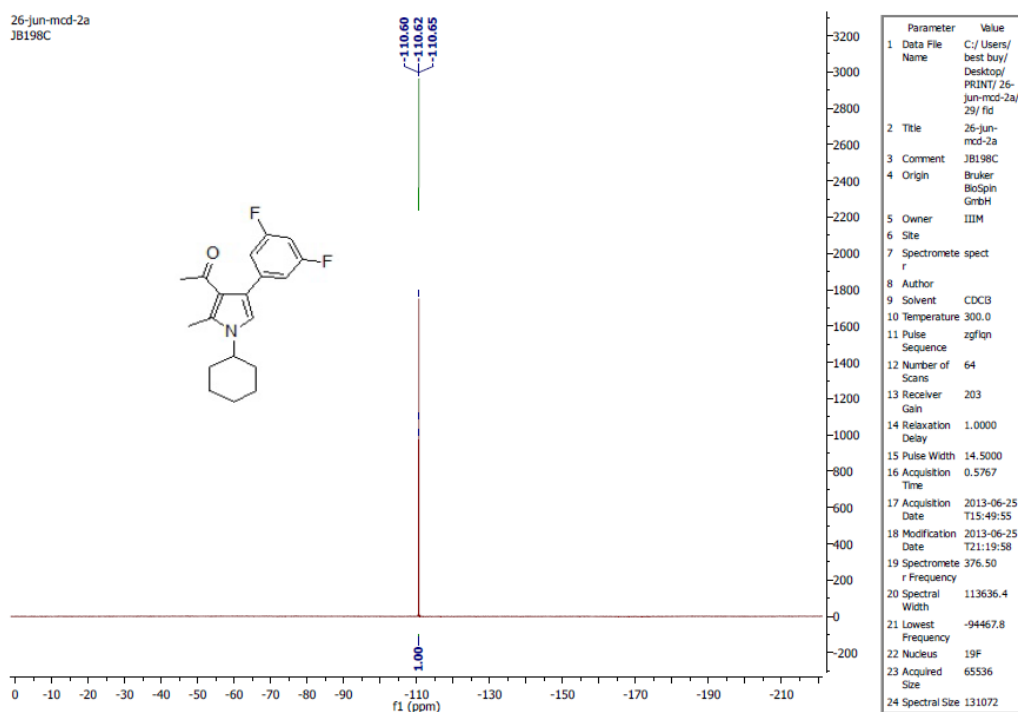
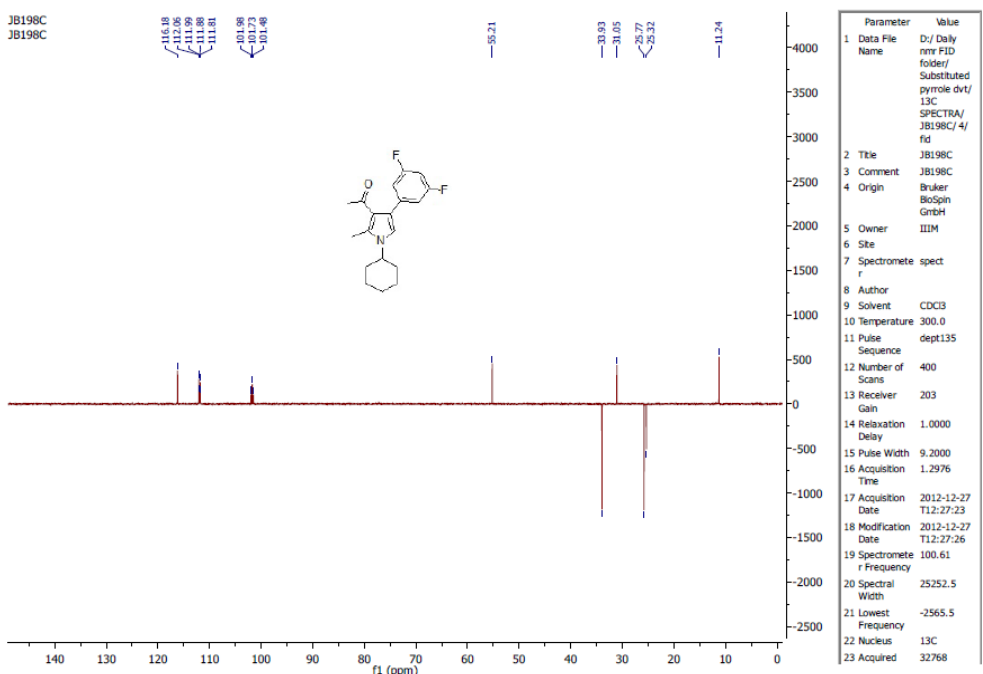
S2.n. ^1H , ^{13}C and DEPT-135 NMR of 1-(1-cyclohexyl-4-(4-methoxyphenyl)-2-methyl-1H-pyrrol-3-yl)ethanone (**1n**)



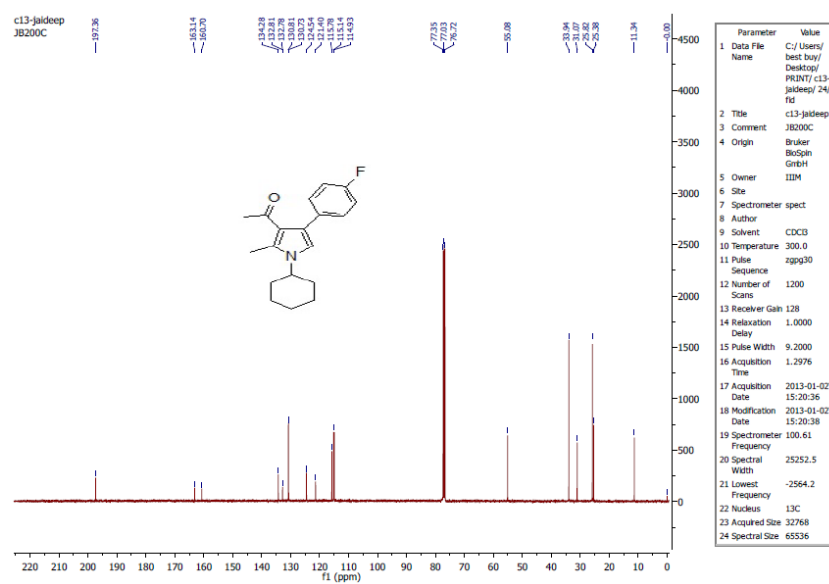
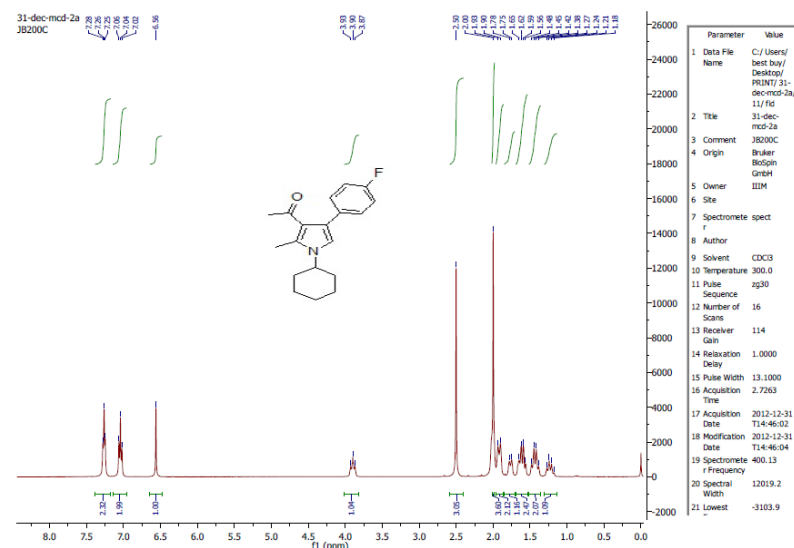


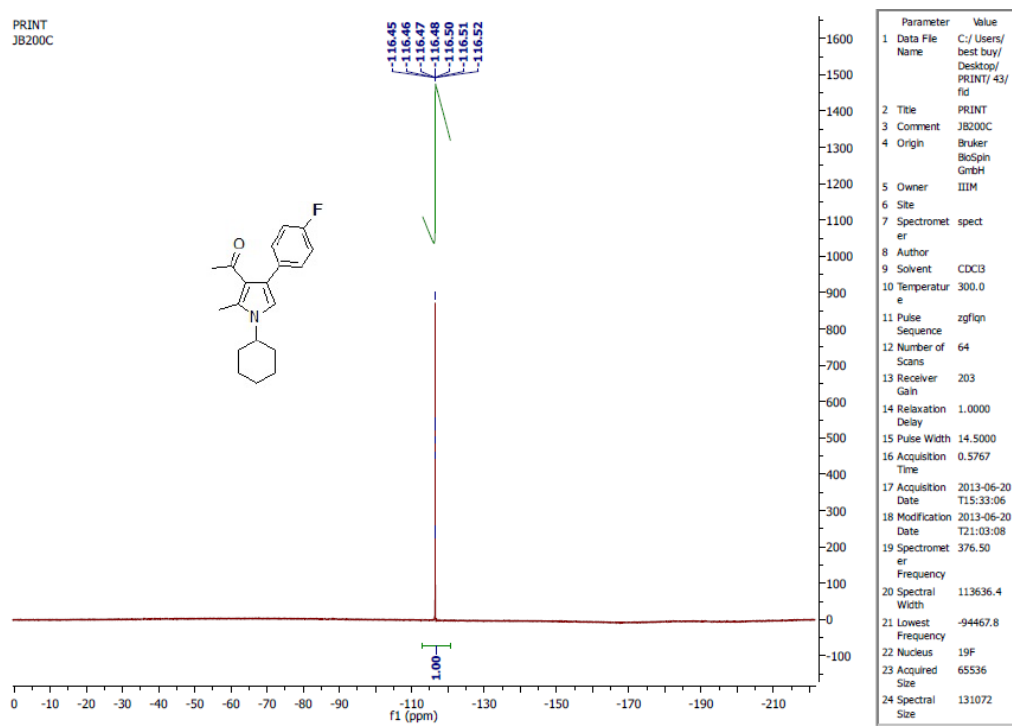
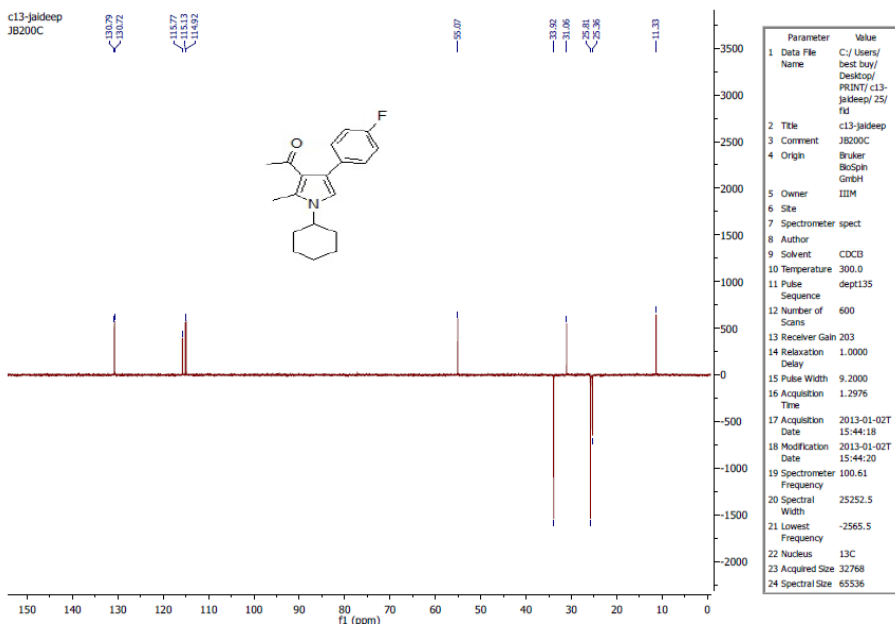
S2.o. ^1H , ^{13}C , DEPT-135 and ^{19}F NMR of 1-(1-cyclohexyl-4-(3,5-difluorophenyl)-2-methyl-1*H*-pyrrol-3-yl)ethanone (**1o**)



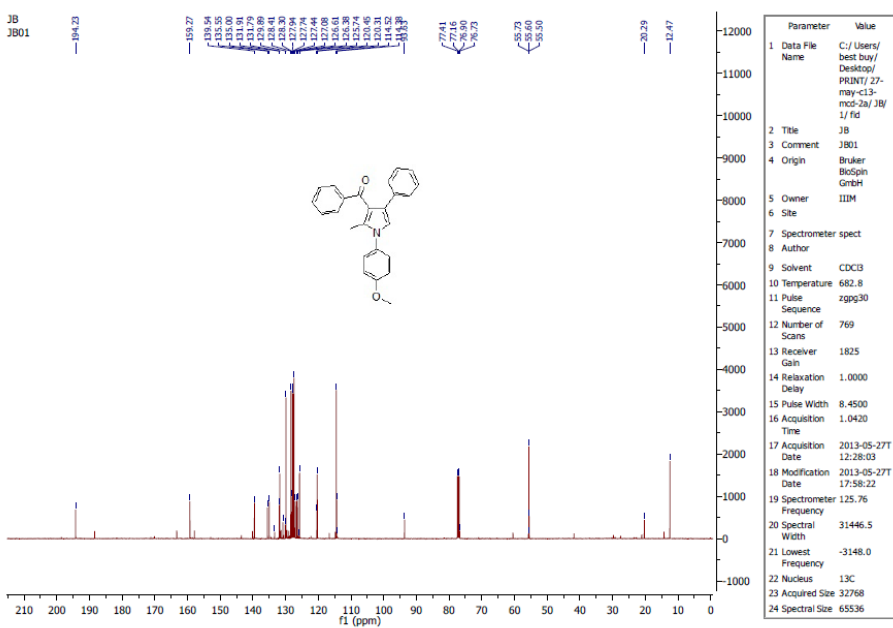
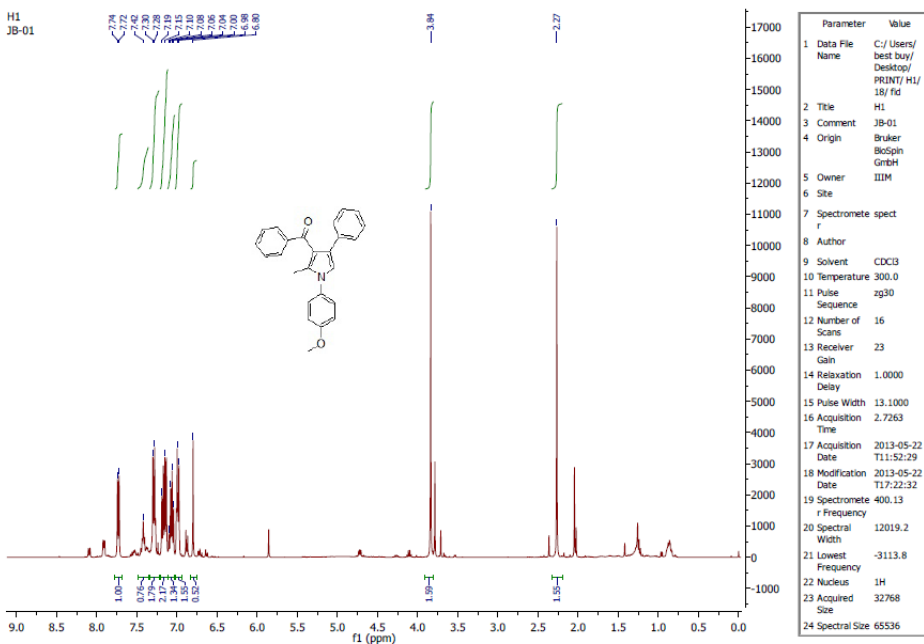


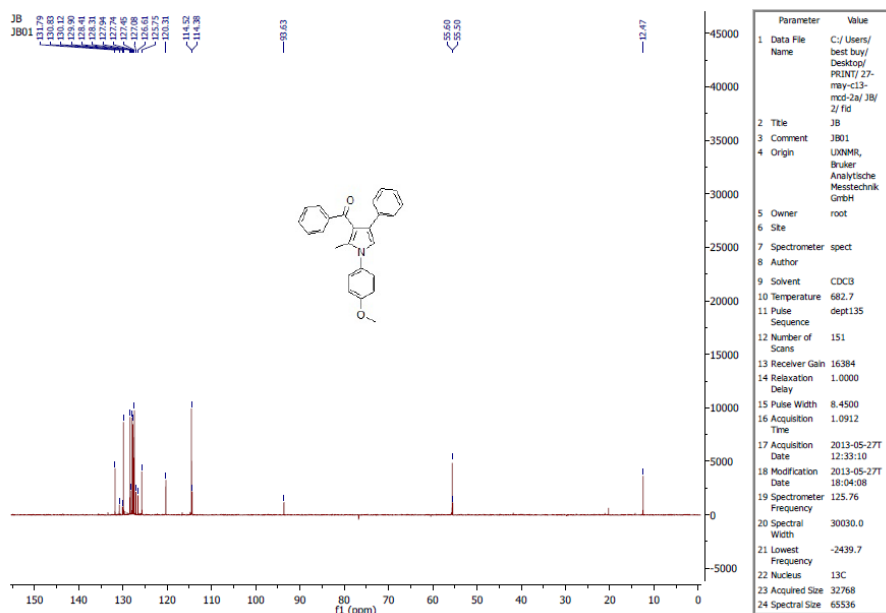
S2.p. ^1H , ^{13}C , DEPT-135 and ^{19}F NMR of 1-(1-cyclohexyl-4-(4-fluorophenyl)-2-methyl-1H-pyrrol-3-yl)ethanone (1p)





S2.q. ^1H , ^{13}C and DEPT-135 NMR of (1-(4-methoxyphenyl)-2-methyl-4-phenyl-1*H*-pyrrol-3-yl)(phenyl)methanone (**1q**)





S3. X-ray crystallography of methyl 1-(1-(4-fluorophenyl)-2-methyl-4-phenyl-1H-pyrrol-3-yl) ethanone 1b:

Single crystals of 1-(1-(4-Fluorophenyl)-2-methyl-4-phenyl-1H-pyrrol-3-yl) ethanone were obtained by slow evaporation at room temperature, from a mixture of Methanol/water. The X-ray data was collected from a dry crystal mounted on an 'Xcalibur, Sapphire3', Oxford diffractometer. The crystal structure was solved by direct method using SHELXS-97 followed by Full matrix anisotropic least square refinement using SHELXL-97. All the hydrogen atoms were located from difference Fourier map and refined isotropically. All the relevant crystallographic data collection parameters and structure refinement details for **1b** is summarized in Table S2. Bond lengths and bond angles are given in Table S3.

Table S2. Crystal data and structure refinement for **1b**

Identification code	1
Empirical formula	C ₁₉ H ₁₆ F ₁ N ₁ O ₁
Formula weight	293.33
Temperature	293(2) K
Wavelength	0.71073 Å
Crystal system	Monoclinic
Space group	P 2 ₁ /n
Unit cell dimensions	a = 9.7980(13) Å α= 90° b = 7.8015(9) Å β= 98.077(13)° c = 20.558(2) Å γ = 90°
Volume	1555.8(3) Å ³
Z	4
Density (calculated)	1.252 Mg/m ³
Absorption coefficient	0.085 mm ⁻¹
F(000)	616
Crystal size	0.4 x 0.2 x 0.2 mm ³
Theta range for data collection	3.75 to 27.00°
Index ranges	-12 ≤ h ≤ 9, -9 ≤ k ≤ 5, -15 ≤ l ≤ 26
Reflections collected	6121
Scan type	ω-scan

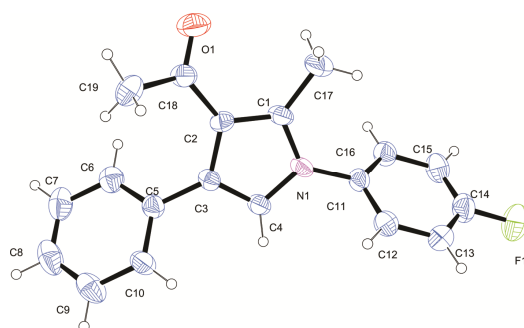
Unique reflections	3330 [R _{int} = 0.0276]
Observed reflection [F > 4σ(F)]	1792
Completeness to theta = 26.74°	98.5 %
Refinement method	Full-matrix least-squares on F ²
Data / restraints / parameters	3330 / 0 / 264
Goodness-of-fit (S)	1.019
Final R indices [I > 2sigma(I)]	R ₁ = 0.0510, wR ₂ = 0.1129
R indices (all data)	R ₁ = 0.1052, wR ₂ = 0.1476
Largest diff. peak and hole	0.136 and -0.140 eÅ ⁻³
CCDC number	946744

Table S3. Bond lengths [Å] and angles [°] for **1b**

H(4) - C(12)	1.00(3)	H(5) - C(4)	0.94(3)
H(2) - C(15)	1.00(3)	H(6) - C(6)	1.01(2)
H(10) - C(10)	1.05(3)	H(15) - C(17)	0.99(3)
H(8) - C(8)	0.94(3)	H(9) - C(9)	0.98(3)
H(16) - C(17)	0.97(4)	H(14) - C(17)	1.02(3)
H(11) - C(19)	0.95(3)	H(1) - C(16)	0.94(3)
H(3) - C(13)	0.93(3)	H(7) - C(7)	1.01(3)
H(12) - C(19)	0.89(4)	H(13) - C(19)	0.90(4)
N(1) - C(1)	1.371(3)	N(1) - C(4)	1.377(3)
N(1) - C(11)	1.425(3)	O(1) - C(18)	1.215(3)
F(1) - C(14)	1.354(4)	C(1) - C(2)	1.383(3)
C(1) - C(17)	1.491(4)	C(2) - C(3)	1.442(3)
C(2) - C(18)	1.464(3)	C(3) - C(4)	1.348(3)
C(3) - C(5)	1.471(3)	C(5) - C(6)	1.385(3)
C(5) - C(10)	1.391(4)	C(6) - C(7)	1.381(4)
C(7) - C(8)	1.368(5)	C(8) - C(9)	1.367(5)
C(9) - C(10)	1.372(5)	C(11) - C(12)	1.379(4)
C(11) - C(16)	1.377(4)	C(12) - C(13)	1.372(4)
C(13) - C(14)	1.350(4)	C(14) - C(15)	1.366(4)
C(15) - C(16)	1.376(4)	C(18) - C(19)	1.496(4)

C(1)-N(1)-C(4) 109.3(2) C(1)-N(1)-C(11) 127.2(2)

C(4)-N(1)-C(11)	123.4(2)	N(1)-C(1)-C(2)	107.4(2)
N(1)-C(1)-C(17)	121.8(2)	C(2)-C(1)-C(17)	130.6(2)
C(1)-C(2)-C(3)	107.2(2)	C(1)-C(2)-C(18)	123.3(2)
C(3)-C(2)-C(18)	129.0(2)	C(2)-C(3)-C(4)	106.8(2)
C(2)-C(3)-C(5)	128.5(2)	C(4)-C(3)-C(5)	124.2(2)
H(5)-C(4)-N(1)	119.2(12)	H(5)-C(4)-C(3)	131.5(12)
N(1)-C(4)-C(3)	109.2(2)	C(3)-C(5)-C(6)	120.9(2)
C(3)-C(5)-C(10)	120.9(2)	C(6)-C(5)-C(10)	118.1(3)
H(6)-C(6)-C(5)	118.8(11)	H(6)-C(6)-C(7)	120.6(11)
C(5)-C(6)-C(7)	120.6(3)	H(7)-C(7)-C(6)	114.1(14)
H(7)-C(7)-C(8)	125.7(14)	C(6)-C(7)-C(8)	120.3(3)
H(8)-C(8)-C(7)	119.4(16)	H(8)-C(8)-C(9)	120.8(16)
C(7)-C(8)-C(9)	119.9(3)	H(9)-C(9)-C(8)	122.0(15)
H(9)-C(9)-C(10)	117.5(15)	C(8)-C(9)-C(10)	120.5(3)
H(10)-C(10)-C(5)	119.3(14)	H(10)-C(10)-C(9)	120.0(14)
C(5)-C(10)-C(9)	120.7(3)	N(1)-C(11)-C(12)	119.0(2)
N(1)-C(11)-C(16)	120.8(2)	C(12)-C(11)-C(16)	120.1(3)
H(4)-C(12)-C(11)	121.7(12)	H(4)-C(12)-C(13)	118.3(12)
C(11)-C(12)-C(13)	120.1(3)	H(3)-C(13)-C(12)	121.5(18)
H(3)-C(13)-C(14)	119.9(18)	C(12)-C(13)-C(14)	118.6(3)
F(1)-C(14)-C(13)	118.9(3)	F(1)-C(14)-C(15)	118.0(3)
C(13)-C(14)-C(15)	123.0(3)	H(2)-C(15)-C(14)	121.2(14)
H(2)-C(15)-C(16)	120.4(14)	C(14)-C(15)-C(16)	118.4(3)
H(1)-C(16)-C(11)	118.3(14)	H(1)-C(16)-C(15)	121.9(14)
C(11)-C(16)-C(15)	119.8(3)	H(15)-C(17)-H(16)	105.5(23)
H(15)-C(17)-H(14)	116.0(21)	H(15)-C(17)-C(1)	111.3(15)
H(16)-C(17)-H(14)	104.8(23)	H(16)-C(17)-C(1)	111.2(17)
H(14)-C(17)-C(1)	107.8(16)	O(1)-C(18)-C(2)	121.8(3)
O(1)-C(18)-C(19)	119.0(3)	C(2)-C(18)-C(19)	119.1(3)
H(11)-C(19)-H(12)	106.1(28)	H(11)-C(19)-H(13)	107.8(27)
H(11)-C(19)-C(18)	114.4(18)	H(12)-C(19)-H(13)	113.8(31)
H(12)-C(19)-C(18)	110.6(23)	H(13)-C(19)-C(18)	104.4(20)



The ORTEP diagram showing numbering scheme and the molecular conformation of **1b** in crystals.